FROM RESEARCH TO INDUSTRY

cea

www.cea.fr

SELF-CONSISTENT MULTIPARTICLE-MULTIHOLE CONFIGURATION MIXING

Nathalie Pillet	CEA/DAM/DIF, France
Caroline Robin	Western Michigan University, USA
Guillaume Hupin	CEA/DAM/DIF, France
Marc Dupuis	CEA/DAM/DIF, France
Luis Robledo	Universidad Autonoma de Madrid
Etienne Caurier	IPHC, France
Jean-François Berger	CEA/DAM/DIF, France
Vladimir Zelevinsky	Michigan state University, USA
Daniel Peña Arteaga	
Julien Le Bloas	

"Pertinent ingredients for MR EDF calculations"

February 27th – March 2nd 2017, ESNT, CEA Saclay , France

SELF-CONSISTENT MULTIPARTICLE-MULTIHOLE CONFIGURATION MIXING

I. General overview

- ✓ General context
- ✓ Link with Green's functions: Exact solution
- ✓ Optimization of orbitals: Truncated solution

II. Numerical algorithm with orbital optimization

- ✓ ^{12}C test nucleus

III. Various applications with the Gogny force

- ✓ Structure: sd-shell nuclei
- ✓ Reactions: (e,e') and (p,p') inelastic scattering

IV. Conclusion and perspectives

- ✓ Derivation of an effective interaction
- ✓ Complex scaling
- ✓ Fitting of a generalized Gogny interaction
- ✓ Effective operators

SELF-CONSISTENT MULTIPARTICLE-MULTIHOLE CONFIGURATION MIXING

I. General overview

- ✓ General context
- ✓ Link with Green's functions: Exact solution
- ✓ Optimization of orbitals: Truncated solution

II. Numerical algorithm with orbital optimization

- ✓ ^{12}C test nucleus

III. Various applications with the Gogny force

- ✓ Structure: sd-shell nuclei
- ✓ Reactions: (e,e') and (p,p') inelastic scattering

IV. Conclusion and perspectives

- ✓ Derivation of an effective interaction
- ✓ Complex scaling
- ✓ Fitting of a generalized Gogny interaction
- ✓ Effective operators

GENERAL OVERVIEW

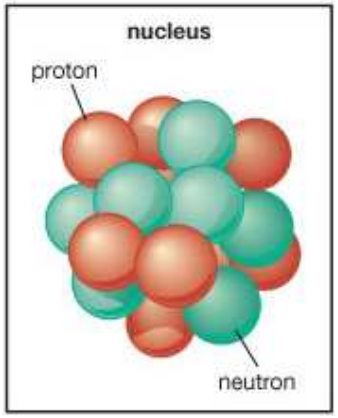

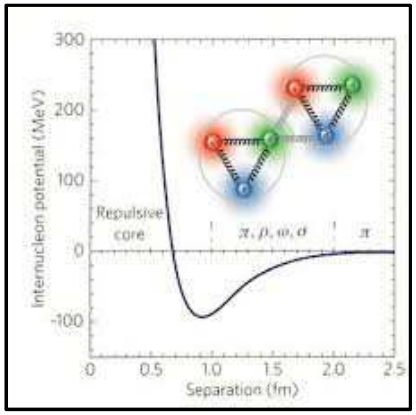

Strongly interacting system

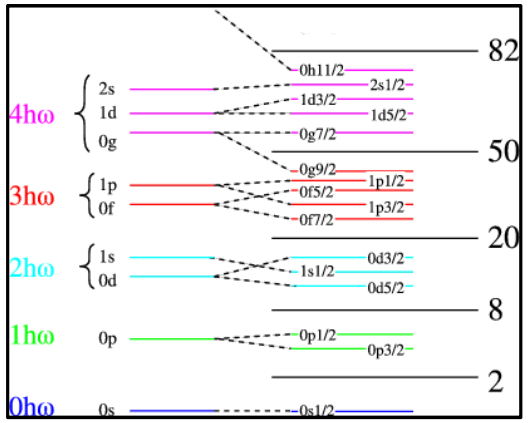

Emergence of a mean-field
(hard core absorbed)

Two step method:

1) **Prerequisite : Existence of a mean-field as rich as possible** (HF for example)

- From phenomenological effective interaction (Gogny)
- From effective interaction derived from bare interactions (MPMH)

⇨ Strongly repulsive core has been avoided/treated

2) **MPMH configuration mixing : nuclear long range correlations**

- Mean-field and beyond
- *Ab initio*

⇨ **Multifaceted approach**

GENERAL OVERVIEW

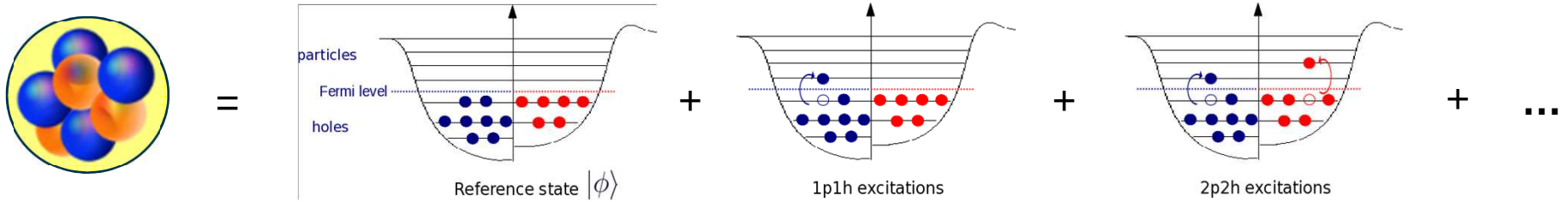

Symmetries and Conservations

- Many-body wave function
- N+Z nucleons
- J conserved
- π conserved
- Fully antisymmetrized (Pauli)

$$|\Phi\rangle = \sum_{\alpha} A_\alpha |\phi_\alpha\rangle$$

Mixing coefficients
(α : proton&neutron dependencies)

Slater determinants
α : MPMH configurations
N+Z nucleons
m-scheme: J_z, T_z
π conserved

Additional properties

- Even-even, odd and odd-odd nuclei
- All types of nuclear long range correlations, deformations

Applications

- Structure : Excitation energies, transition probabilities, masses, radii, …
- Reactions : Inelastic nucleon and electron scattering, resonances
- Tool to test effective interactions and generate effective interactions from bare/chiral forces

GENERAL OVERVIEW

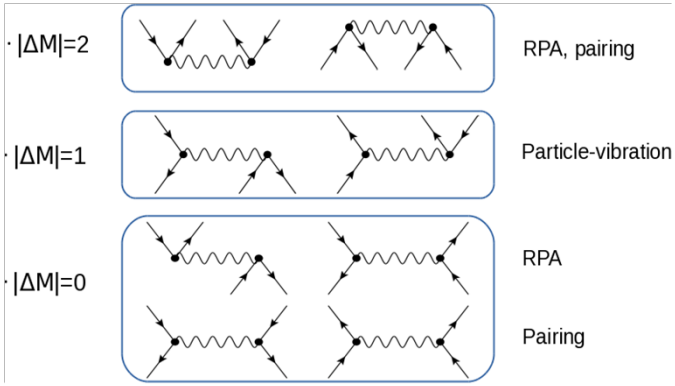

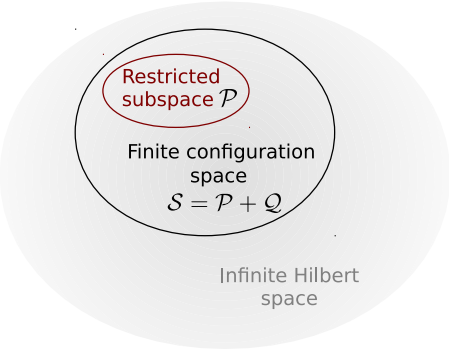

Hamiltonian (extension to three-body straightforward)

$$\hat{H} = \sum_{ij} K_{ij}\ a_i^\dagger a_j + \frac{1}{4}\sum_{ijkl} \widetilde{V}^{2N}_{ijkl}\ a_i^\dagger a_j^\dagger a_l a_k$$

Many-body wave function

- Full Hilbert space $|\Psi_{ex}\rangle$
- Truncated Hilbert space $|\Psi\rangle$

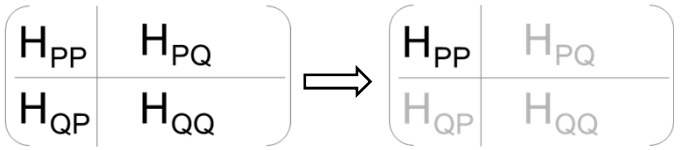

Variational principal on the total energy $\mathcal{E}[\Psi_{(ex)}] = \langle\Psi_{(ex)}|\hat{H}|\Psi_{(ex)}\rangle$

$$\delta_A\{\mathcal{E}[\Psi_{(ex)}] - \lambda\langle\Psi_{(ex)}|\Psi_{(ex)}\rangle\} = 0 \iff \sum_\beta \langle\phi_\alpha|\hat{H}|\phi_\beta\rangle\, A_\beta = \lambda A_\alpha$$

⇒ **Mixing coefficients determined**

⇒ **What about orbitals?**

GENERAL OVERVIEW

Link with Green's functions : Exact solution $|\Psi_{ex}\rangle$

- **One and two-body Green's functions**

$$\mathcal{G}^{[1]}_{ij}(t_1 - t_2) = -i \langle \Psi_{ex} | \mathcal{T} \left(a_i(t_1) a^\dagger_j(t_2) \right) | \Psi_{ex} \rangle$$

$$\mathcal{G}^{[2]}_{ijkl}(t_1, t_2; t_3, t_4) = - \langle \Psi_{ex} | \mathcal{T} \left(a_i(t_1) a_j(t_2) a^\dagger_l(t_4) a^\dagger_k(t_3) \right) | \Psi_{ex} \rangle$$

- **Equation of motion of the one-body propagator**

$$\sum_k \left(-K_{ik} \mathcal{G}^{[1]}_{kj}(t - t') + \mathcal{G}^{[1]}_{ik}(t - t') K_{kj} \right) = \frac{i}{2} \sum_{klm} \widetilde{V}^{2N}_{iklm} \mathcal{G}^{[2]}_{mljk}(t, t; t', t^+) + \frac{i}{2} \sum_{klm} \widetilde{V}^{2N}_{klmj} \mathcal{G}^{[2]}_{imlk}(t, t'^-; t', t')$$

- **Equal time limit $t' \to t^+$**

$$\lim_{t' \to t^+} \mathcal{G}^{[1]}_{kj}(t - t') = -i \langle \Psi_{ex} | T \left(a_k(t) a^\dagger_j(t^+) \right) | \Psi_{ex} \rangle = +i \rho_{kj} \ ,$$

$$\lim_{t' \to t^+} \mathcal{G}^{[2]}_{mljk}(t, t; t', t^+) = - \langle \Psi_{ex} | T \left(a_m(t) a_l(t) a^\dagger_k(t^+) a^\dagger_j(t^+) \right) | \Psi_{ex} \rangle = + \langle \Psi_{ex} | a^\dagger_j a^\dagger_k a_m a_l | \Psi_{ex} \rangle = \rho_{lj} \rho_{mk} - \rho_{lk} \rho_{mj} + \sigma_{jl,km}$$

⟹ **Getting of the orbital equation**

GENERAL OVERVIEW

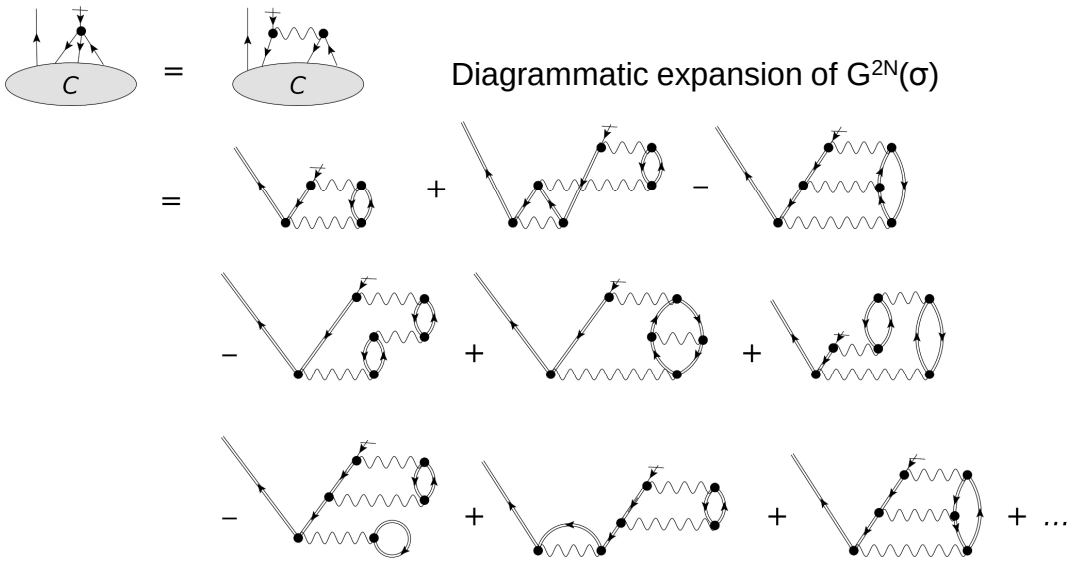

Diagrammatic expansion of $G^{2N}(\sigma)$

General mean-field h(ρ)

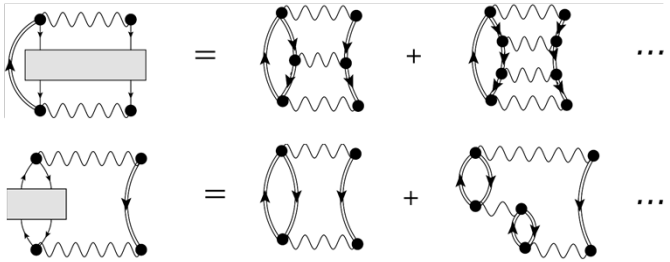

Particular cases: Resummation of ladder and ring diagrams in $G^{2N}(\sigma)$

Link with Green's functions : Orbital equation

$$\left[\hat{h}[\rho], \hat{\rho}\right] = \hat{G}[\sigma]$$

- Connected part of the two-body density
- Source term
- General mean-field
- Correlated one-body density

$$\hat{h}[\rho]_{ij} \equiv K_{ij} + \Gamma^{2N}[\rho]_{ij} = K_{ij} + \sum_{kl} \widetilde{V}^{2N}_{ikjl}\ \rho_{lk} \qquad G[\rho,\sigma] = F[\sigma] - F^{\dagger}[\sigma] \text{ with } F[\sigma]_{ij} = \frac{1}{2}\sum_{klm} \sigma_{ki,lm}\widetilde{V}^{2N}_{kljm}$$

⇨ Equation automatically satisfied in the case of exact solution!

GENERAL OVERVIEW

Link with the self-energy

- **Self-energy** $\Sigma(t-t') = \Sigma^{[0]}\delta(t-t') + \Sigma^{dyn}(t-t')$

  static dynamic

- **Average potential and static part of the self-energy**

$$\Sigma^{[0]} = \Gamma^{2N}[\rho]$$

- **Source term and dynamic part of the self-energy**

Cluster expansion:

$$\begin{aligned}&\mathcal{G}^{[2]}_{ijkl}(t_1,t_2;t_3,t_4)\\ &= \mathcal{G}^{[1]}_{ik}(t_1-t_3)\mathcal{G}^{[1]}_{jl}(t_2-t_4) - \mathcal{G}^{[1]}_{il}(t_1-t_4)\mathcal{G}^{[1]}_{jk}(t_2-t_3)\\ &\quad + \mathcal{G}^{[2]C}_{ijkl}(t_1,t_2;t_3,t_4)\end{aligned}$$

$$\Sigma^{dyn}_{ij}(t-t') = -i\int dt_1 \sum_{klmn} \widetilde{V}^{2N}_{kilm}\mathcal{G}^{[2]C}_{mlnk}(t,t;t_1,t^+)\mathcal{G}^{[1]-1}_{nj}(t_1-t')$$

$$\lim_{t_2\to t_1^+}\sum_s \int dt' \Sigma^{dyn}_{is}(t_1-t')\mathcal{G}^{[1]}_{sj}(t'-t_2) = \frac{i}{2}\sum_{klm}\widetilde{V}^{2N}_{kilm}\,\sigma_{kl,jm} = i(\hat{F}^\dagger)_{ij}$$

GENERAL OVERVIEW

Caroline Robin
PhD at CEA/DAM/DIF
Postdoc at WMU

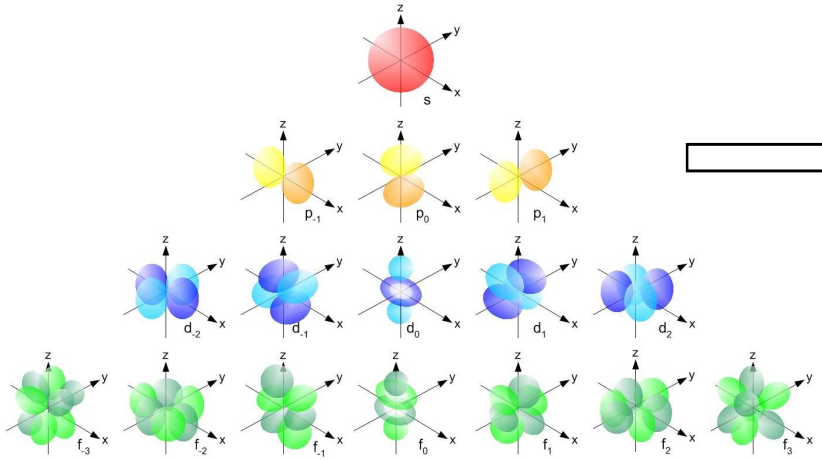

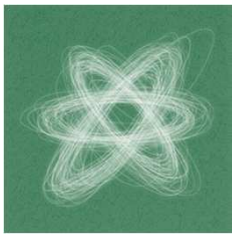

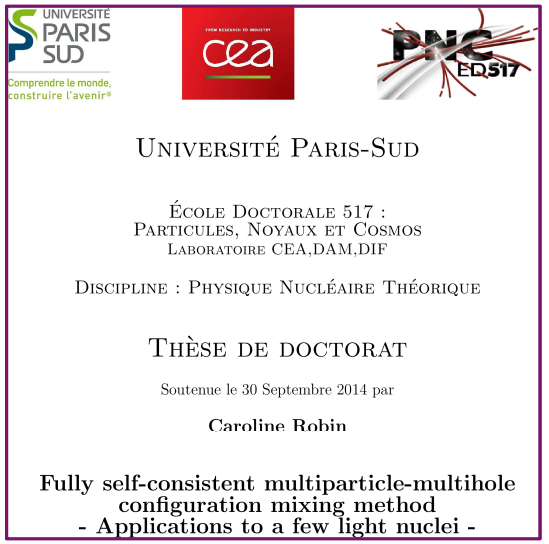

UNIVERSITÉ PARIS SUD
Comprendre le monde, construire l'avenir®

UNIVERSITÉ PARIS-SUD

ÉCOLE DOCTORALE 517 :
PARTICULES, NOYAUX ET COSMOS
LABORATOIRE CEA,DAM,DIF

DISCIPLINE : PHYSIQUE NUCLÉAIRE THÉORIQUE

THÈSE DE DOCTORAT

Soutenue le 30 Septembre 2014 par

Caroline Robin

Fully self-consistent multiparticle-multihole configuration mixing method - Applications to a few light nuclei -

Optimization of Orbitals : Truncated solution $|\Psi\rangle$

- **Minimization of the total energy**

$\Longrightarrow$ First order variation (unitary trar$\mathcal{E}[\Psi]$hation): Brillouin condition

$$\delta_\varphi \mathcal{E}[\Psi] = 0 \Leftrightarrow \left[\hat{h}[\rho], \hat{\rho}\right] = \hat{G}[\sigma]$$

$\Longrightarrow$ Orbital equation similar to the one derived with the exact solution but not satisfied automatically!

$\Longrightarrow$ **Need to establish the consistency between one- and two-body properties by solving explicitly the orbital equation**

GENERAL OVERVIEW

Truncations and Symmetries

- **Truncations compatible with the conservation of the advantages of the method**
  - ✓ Conservation of desired symmetries
  - ✓ All types of nuclear long range correlations, deformations
  - ✓ Even-even, odd and odd-odd nuclei
  - ✓ Full antisymmetrization (Pauli)

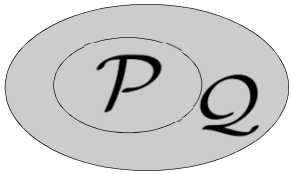

- **Different possible truncations $\Longrightarrow$ Flexibility of the MPMH configuration mixing**
  - ✓ Core+valence space
  - ✓ Excitation order of the configurations
  - ✓ Excitation energy of the configurations

  $\Longrightarrow$ Ideally, a combination of the truncations with the preservation of desired symmetries
  $\Longrightarrow$ Systematically improvable method

- **Symmetries**
  - ✓ Unitary operator $U = e^{\hat{J}\theta}$ such that: $U\hat{K}U^{-1} = \hat{K}, \quad U\hat{V}^{2N}U^{-1} = \hat{V}^{2N}$
  - ✓ Transformed single-particle states: $|\bar{i}\rangle = U|i\rangle$
  - ✓ General mean field

GENERAL OVERVIEW

✓ General mean-field

$$\begin{aligned}\langle i|h|j\rangle &= \langle i|K|j\rangle + \sum_{kl}\langle il|\widetilde{V}^{2N}|jk\rangle\ \langle k|\rho|l\rangle \\ &= \langle i|UKU^{-1}|j\rangle + \sum_{kl}\langle il|U\widetilde{V}^{2N}U^{-1}|jk\rangle\ \langle k|\rho|l\rangle \\ &= \langle \bar{i}|K|\bar{j}\rangle + \sum_{kl}\langle \bar{i}\ \bar{l}|\widetilde{V}^{2N}|\bar{j}\ \bar{k}\rangle\ \langle k|\rho|l\rangle\end{aligned}$$

The summation on transformed states can be replaced by a summation on the states k and l. Hence,

$$\langle i|h|j\rangle = \langle \bar{i}|K|\bar{j}\rangle + \sum_{kl}\langle \bar{i}l|\widetilde{V}^{2N}|\bar{j}k\rangle\ \langle \bar{k}|\rho|\bar{l}\rangle$$

If $\langle \bar{k}|\rho|\bar{l}\rangle = \langle k|\rho|l\rangle$ or equivalently $U\hat{\rho}U^{-1} = \hat{\rho}$, then

$$\langle \bar{k}|\hat{h}|\bar{l}\rangle = \langle k|\hat{h}|l\rangle \iff UhU^{-1} = h$$

⟹ **Of course, the equality will depend on the mixing introduced in the N-body wave function!**

GENERAL OVERVIEW

Importance of the consistency between correlations and mean-field description

- Most microscopic N-body methods are based on the concept of an existing underlying independent-particle picture
- The inclusion of correlations arising from the residual interaction is accomplished in a second separate stage

⟹ The MPMH configuration mixing allows to generate an optimized single-particle picture which reflects and encapsulates part of the correlations content of the system

$$h[\rho]_{ij} = K_{ij} + \Gamma^{2N}[\rho]_{ij} = K_{ij} + \sum_{kl} \langle ik|\widetilde{V}^{2N}|jl\rangle\, \rho_{lk}$$

Contrary to the HF approximation, both particle and hole states participate to the definition of *h*.

- Average potential from M-body forces: folding of the N-body interactions with the full (n-1)-body densities (0<n<M+1)

$$\begin{aligned} h_{ij}[\rho, \rho^{[2]}, ..., \rho^{[M-1]}] \;=\; & K_{ij} + \sum_{kl} \langle ik|\widetilde{V}^{2N}|jl\rangle\, \rho_{lk} + \frac{1}{4} \sum_{k_1 l_1 k_2 l_2} \langle ik_1k_2|\widetilde{V}^{3N}|jl_1l_2\rangle\, \rho^{[2]}_{l_1k_1,l_2k_2} \\ & + ... + \frac{1}{(M-1)!^2} \sum_{k_1 l_1 ... k_M l_M} \langle ik_1...k_M|\widetilde{V}^{MN}|jl_1...l_M\rangle\, \rho^{[M-1]}_{l_1k_1,...,l_{M_1}k_{M-1}} \end{aligned}$$

The average potential absorbs the mean effect of correlations and partly shields their influence

⟹ The influence of the residual interaction is then minimized and the independent-particle system governed by *h* should be a better approximation to the exact solution than the HF state.

GENERAL OVERVIEW

- Expression of such a potential extensively discussed by Baranger and more recently by Duguet et al. in the context of definition of single-particle energies ε .

$$\Longrightarrow \varepsilon_a = \langle a|h[\rho]|a\rangle = K_{aa} + \sum_{bc} \langle ab|\widetilde{V}^{2N}|ac\rangle\, \rho_{cb} \qquad \text{where} \quad h[\rho]\,|a\rangle = \varepsilon_a\,|a\rangle$$

$\Longrightarrow$ Eigenvalues of the general mean-field: « Universal » unambiguous definition of the single-particle energies which also coincides with the « experimentalist » definition.

Indeed:

$$\hat{h}[\rho]_{ij} = \langle\Psi|\left\{\left[a_i, \hat{H}\right], a_j^\dagger\right\}|\Psi\rangle$$

Using the closure relations

$$\hat{1} = \sum_N |\Psi_N^{A+1}\rangle\langle\Psi_N^{A+1}| = \sum_n |\Psi_n^{A-1}\rangle\langle\Psi_n^{A-1}|$$

Then,

$$\hat{h}[\rho]_{ij} = \sum_N \langle\Psi|a_i|\Psi_N^{A+1}\rangle\,(E_N - E)\,\langle\Psi_N^{A+1}|a_j^\dagger|\Psi\rangle + \sum_n \langle\Psi|a_j^\dagger|\Psi_n^{A-1}\rangle\,(E - E_n)\,\langle\Psi_n^{A-1}|a_i|\Psi\rangle$$

$$\varepsilon_a = h_{aa}[\rho] = \sum_N \left|\langle\Psi_N^{A+1}|a_a^\dagger|\Psi\rangle\right|^2 (E_N - E) + \sum_n \left|\langle\Psi_n^{A-1}|a_a|\Psi\rangle\right|^2 (E - E_n)$$

$\Longrightarrow$ One-nucleon addition and separation energies

$\Longrightarrow$ Spectroscopic factors

Centroids of the observable separation energies

14

GENERAL OVERVIEW

- **Theory of the most general mean-field from the point of view of perturbation theory**

The density ρ used to calculate the potential Γ(ρ) must be fully consistent with the correlations σ of the system

More precisely, on can always divide ρ into an uncorrelated part and a correlated part

$$\rho = \rho^{(0)} + \rho^{(1)}$$

- $\rho^{(0)} = \langle\phi|\hat{\rho}|\phi\rangle$ is the density of the uncorrelated reference state $|\phi\rangle$. It satisfies the equation $(\rho^{(0)})^2 = \rho^{(0)}$, characteristic of an independent-particle state.
- $\rho^{(1)} = \rho - \rho^{(0)}$ is the contribution to the one-body density arising from the two-body correlations. The presence of this part leads to the loss of the idempotence property: $(\rho)^2 \neq \rho$

Using graph expansion of ρ and the total energy E, it can be shown that the variational condition

$$\frac{\delta E[\Gamma]}{\delta \Gamma} = 0$$

is realized if Γ(ρ) is calculated with $\rho^{(1)}$ satisfying:

$$\rho^{(1)} = \frac{\delta}{\delta\Gamma}(\Delta) = \frac{\delta}{\delta\Gamma}(\text{"Irreducible" energy diagrams})$$

⟹ The results stay true in the case where one truncates the infinite summation Δ in the expansion of the energy E, or limits this summation to a certain subclass of diagrams as long as the same graphs are used to calculate $\rho^{(1)}$

⟹ Although the variational principle applied in the MPMH configuration mixing approach is different (explicit expression of the wave function), consistency between the one-body density ρ and the correlation matrix σ is achieved by the fact that they are calculated from the same nuclear state

15

GENERAL OVERVIEW

Role of the self-consistency on N-body configurations

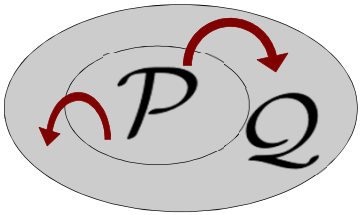

Coupling to the Q-subspace

- **Variation of the many-body state induced by the variation of single-particle states**

$$|\Psi\rangle_{\mathcal{P}} \rightarrow |\Psi\rangle_{\mathcal{P}} + |\delta\Psi\rangle \text{ , where } |\delta\Psi\rangle = |\delta\Psi\rangle_{\mathcal{P}} + |\delta\Psi\rangle_{\mathcal{Q}}$$

- **Variation of the total energy**

$$\begin{aligned}
\delta_\phi \mathcal{E}[\Psi] &= {}_{\mathcal{P}}\langle\Psi|\hat{H}\,|\delta\Psi\rangle + \langle\delta\Psi|\hat{H}|\Psi\rangle_{\mathcal{P}} \\
&= {}_{\mathcal{P}}\langle\Psi|\hat{H}\,|\delta\Psi\rangle_{\mathcal{P}} + {}_{\mathcal{P}}\langle\delta\Psi|\hat{H}\,|\Psi\rangle_{\mathcal{P}} + {}_{\mathcal{P}}\langle\Psi|\hat{H}\,|\delta\Psi\rangle_{\mathcal{Q}} + {}_{\mathcal{Q}}\langle\delta\Psi|\hat{H}\,|\Psi\rangle_{\mathcal{P}} \\
&= {}_{\mathcal{P}}\langle\Psi|\hat{P}\hat{H}\hat{P}\,|\delta\Psi\rangle_{\mathcal{P}} + {}_{\mathcal{P}}\langle\delta\Psi|\hat{P}\hat{H}\hat{P}\,|\Psi\rangle_{\mathcal{P}} + {}_{\mathcal{P}}\langle\Psi|\hat{P}\hat{H}\hat{Q}\,|\delta\Psi\rangle_{\mathcal{Q}} + {}_{\mathcal{Q}}\langle\delta\Psi|\hat{Q}\hat{H}\hat{P}\,|\Psi\rangle_{\mathcal{P}}
\end{aligned}$$

⟹ Couplings between P- and Q-subspaces introduced through $\hat{H}_{\mathcal{QP}} \equiv \hat{Q}\hat{H}\hat{P}$ and $\hat{H}_{\mathcal{PQ}} \equiv \hat{P}\hat{H}\hat{Q}$

⟹ Propagation into the Q-subspace through $\hat{H}_{\mathcal{QQ}} \equiv \hat{Q}\hat{H}\hat{Q}$ is ignored with a first order variation

⟹ Optimal selection criterion of the P-subspace

GENERAL OVERVIEW

- **Role of the orbital equation**

Compensation for the truncations made on the wave function

Starting from a certain set of single-particle states (a+), the orbital equation lead to a new set (b+):

$$b_i^\dagger = e^{i\hat{\Lambda}} a_i^\dagger e^{-i\hat{\Lambda}} = \sum_j a_j^\dagger \left(e^{i\hat{\Lambda}}\right)_{ji} \equiv \sum_j a_j^\dagger \theta_{ji}$$

where $\hat{\Lambda} = \sum_{kl} \Lambda_{kl} a_k^\dagger a_l$

Under this transformation, the N-body configurations vary as

$$\begin{aligned} |\phi_\alpha\rangle \to |\phi'_\alpha\rangle &= e^{i\Lambda}|\phi_\alpha\rangle \\ &= |\phi_\alpha\rangle + \sum_{ij} \Lambda_{ij} a_i^\dagger a_j |\phi_\alpha\rangle + \sum_{ijkl} \Lambda_{ij}\Lambda_{kl} a_i^\dagger a_j a_k^\dagger a_l |\phi_\alpha\rangle + \ldots \end{aligned}$$

⟹ Optimization of orbitals: Creation of MPMH excitations on top of the existing configurations

⟹ The MPMH excitations extend to the whole single-particle basis one is considering

⟹ Since Λ is a one-body operator, they are always built as product of 1P1H excitations

The configurations belonging to the new P'-subspace should take into account the effect of Slater determinants built from the entire starting single-particle basis

$$\begin{aligned} |\phi'_\alpha\rangle &= b_{1_\alpha}^\dagger \ldots b_{A_\alpha}^\dagger |0\rangle \\ &= \sum_{j_1 \ldots j_A} \theta_{j_1 1_\alpha} \ldots \theta_{j_A A_\alpha} a_{j_1}^\dagger \ldots a_{j_A}^\dagger |0\rangle \end{aligned}$$

or

$$|\phi'_\alpha\rangle = \sum_{\substack{\beta \in \mathcal{P}+\mathcal{Q} \\ \text{with same symmetry} \\ \text{than } \alpha'}} C_{\alpha\beta} |\phi_\beta\rangle$$

SELF-CONSISTENT MULTIPARTICLE-MULTIHOLE CONFIGURATION MIXING

I. General overview
- ✓ General context
- ✓ Link with Green's functions: Exact solution
- ✓ Optimization of orbitals: Truncated solution

II. Numerical algorithm with orbital optimization
- ✓ ^{12}C test nucleus

III. Various applications with the Gogny force
- ✓ Structure: sd-shell nuclei
- ✓ Reactions: (e,e') and (p,p') inelastic scattering

IV. Conclusion and perspectives
- ✓ Derivation of an effective interaction
- ✓ Complex scaling
- ✓ Fitting of a generalized Gogny interaction
- ✓ Effective operators

NUMERICAL ALGORITHM WITH ORBITAL OPTIMIZATION

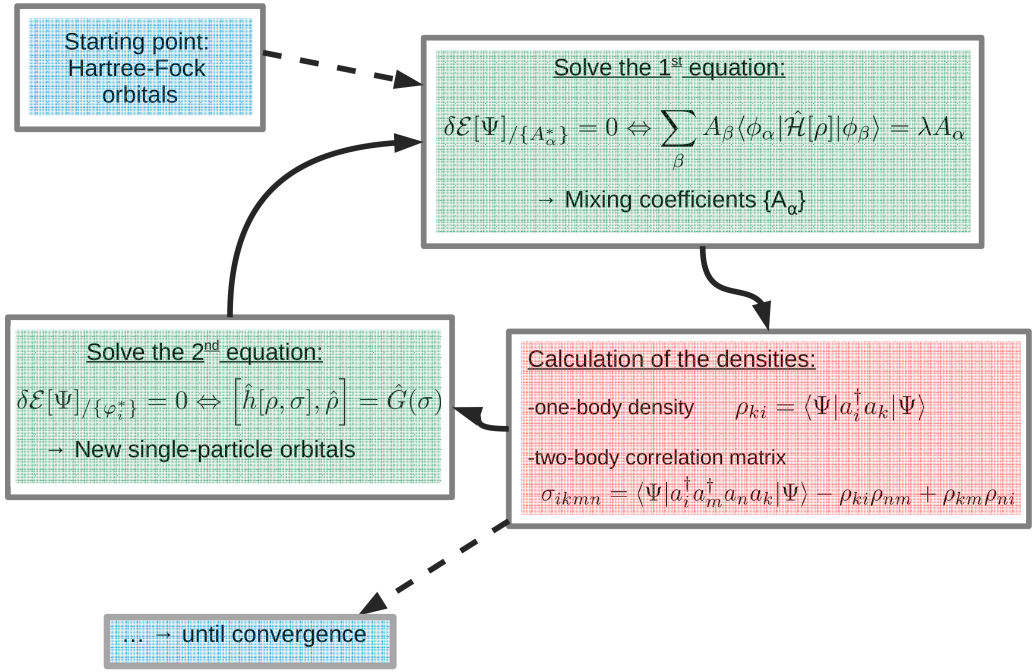

Global iterative procedure

1. Start with the standard HF calculation which assumes a single-configuration wave function $|\Psi^{(0)}\rangle = |\phi^{(0)}\rangle$ so that no correlations are present, $\sigma^{(0)} = 0$ and $\rho^{(0)} = \langle\phi_0|\hat{\rho}|\phi_0\rangle = \rho_0 = \rho_0^2$. Solve the corresponding equation $\left[h\left(\rho^{(0)}\right), \rho^{(0)}\right] = 0$.

2. Construct the many-body configurations $\left\{\phi_\alpha^{(0)}\right\}$ on these initial orbitals and solve 1st equation to obtain a first set of ground state components $\left\{A_\alpha^{(1)}\right\}$ (shell model technique). The matrix density $\sigma^{(1)}$ can then be calculated.

3. Keeping $\sigma^{(1)}$ fixed, solve 2nd equation, to obtain the one-body density $\rho^{(1)}$. The new single-particle states $\left\{\varphi_i^{(1)}\right\}$ are taken as eigenvectors of the solution $\rho^{(1)}$.

4. Go back to step 2. using the new orbitals, and repeat the procedure until convergence is reached.

NUMERICAL ALGORITHM WITH ORBITAL OPTIMIZATION

Solve the 2nd equation:

$$\delta\mathcal{E}[\Psi]_{/\{\varphi_i^*\}} = 0 \Leftrightarrow \left[\hat{h}[\rho,\sigma],\hat{\rho}\right] = \hat{G}(\sigma)$$

→ New single-particle orbitals

Solution of the orbital equation: adopted algorithm

Main idea: $G^{2N}(\sigma) = [Q(\rho,\sigma),\rho]$

The orbital equation in an homogeneous form

- Natural basis

$$\sum_{\alpha\beta}(U^T)_{\mu\alpha}\rho_{\alpha\beta}U_{\beta\upsilon} = n_\mu\delta_{\mu\nu}$$

- Orbital equation in the natural basis

$$h_{\mu\nu}(n_\upsilon - n_\mu) = G_{\mu\nu}$$

  - ✓ No degenracy

    $n_\nu = n_\mu \Longrightarrow \nu = \mu \Longrightarrow G_{\mu\nu} = G_{\mu\mu} = 0$

  - ✓ Degeneracies

    - symmetries
    - core+valence space+empty orbital

    $\Longrightarrow G_{\mu\nu} = 0$

- Correlation field: $Q_{ij}(\rho,\sigma) = \begin{cases} \frac{G_{ij}(\sigma)}{n_j - n_i} & if\ n_i \neq n_j \\ 0 & otherwise \end{cases}$

Solution of the orbital equation

1. Start from an initial correlated one-body density $\rho = \rho_{init}$ and diagonalize it to obtain occupation numbers n_i.

2. Calculate and diagonalize $h(\rho,\sigma) - Q(\rho,\sigma)$. The resulting eigenvectors constitutes new single-particle states.

3. Redistribute the particles on this new basis to obtain a new density ρ.

4. Go back to step 2. …, and so on until the ρ matrix has convergedin a given basis at the desired accuracy

NUMERICAL ALGORITHM WITH ORBITAL OPTIMIZATION

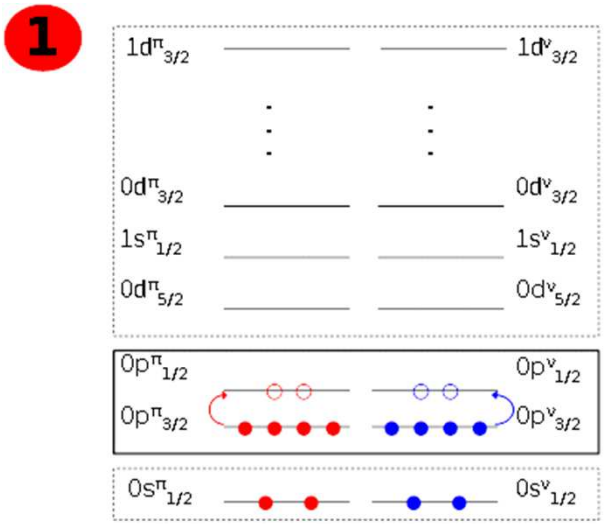

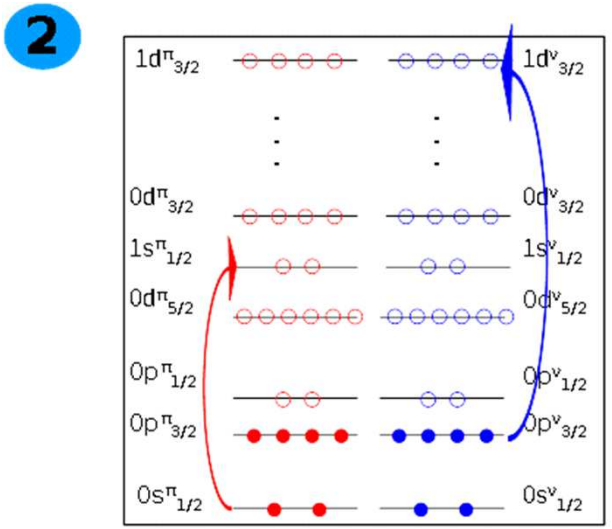

(5 major oscillator shells)

^{12}C test nucleus

Two types of truncation schemes tested:

1. ^{4}He core + 0ħω valence space
   - 38 configurations
   - Natural max. excitation order: 4P4H
2. Nħω space
   - Truncation at 4P4H
   - 26 401 700 configurations

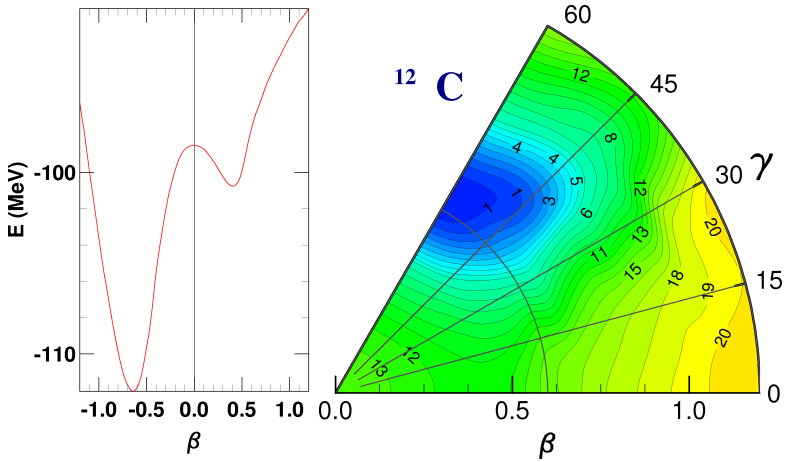

NUMERICAL ALGORITHM WITH ORBITAL OPTIMIZATION

Two-body correlation matrix σ_{ijkl}

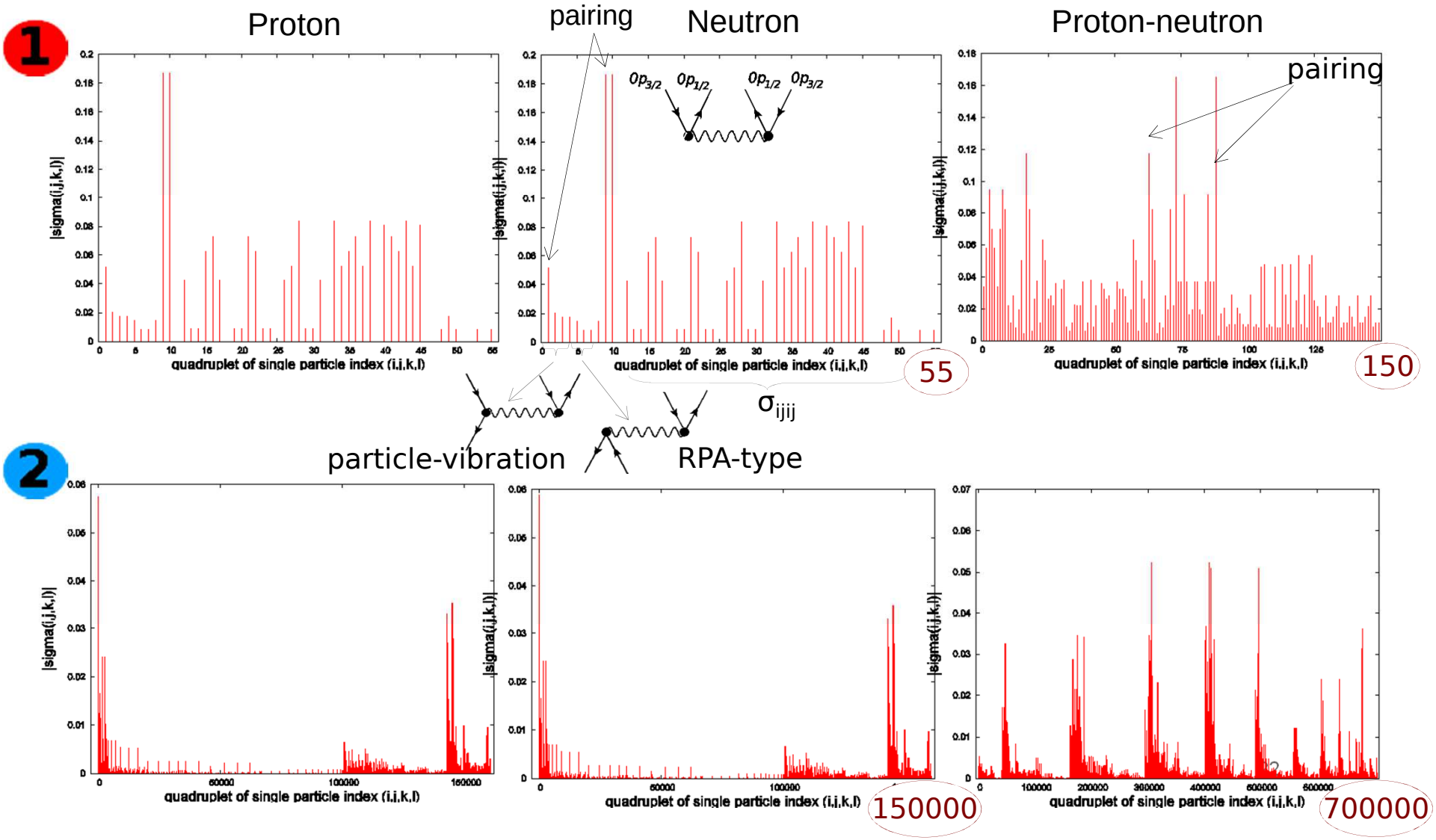

NUMERICAL ALGORITHM WITH ORBITAL OPTIMIZATION

Source term $G(\sigma)_{ij}$

1

Proton

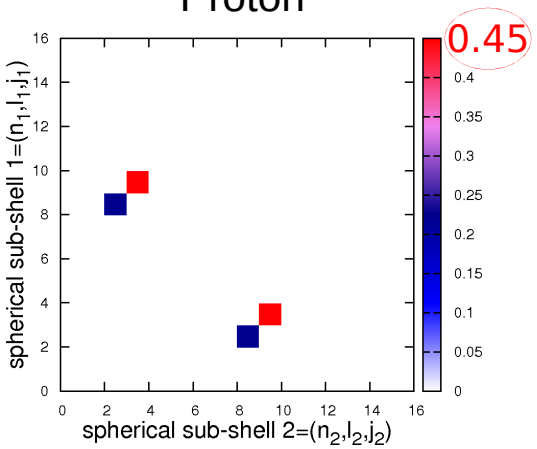

Neutron

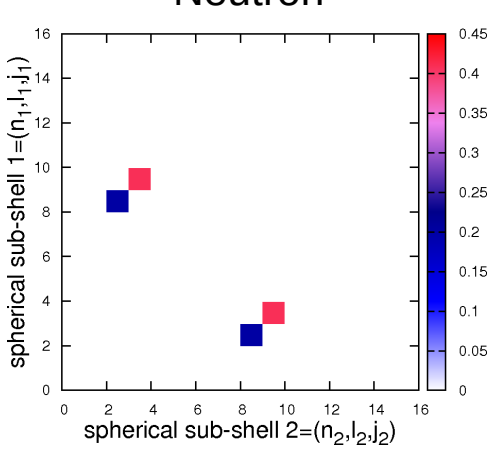

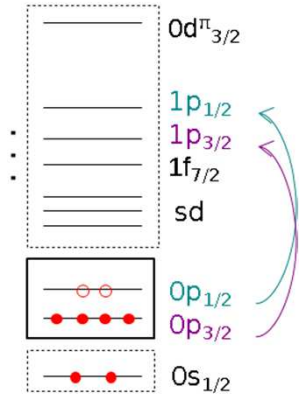

2

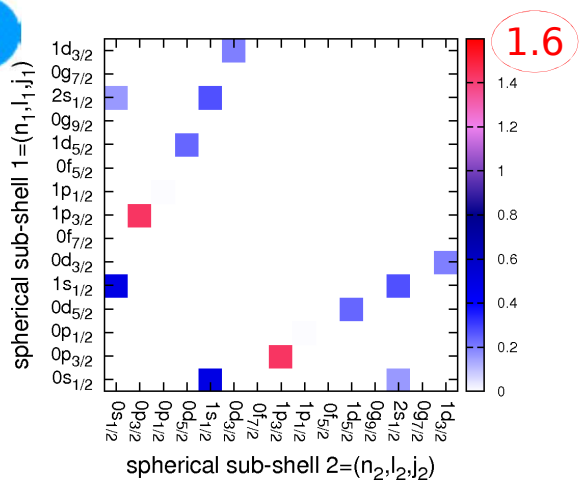

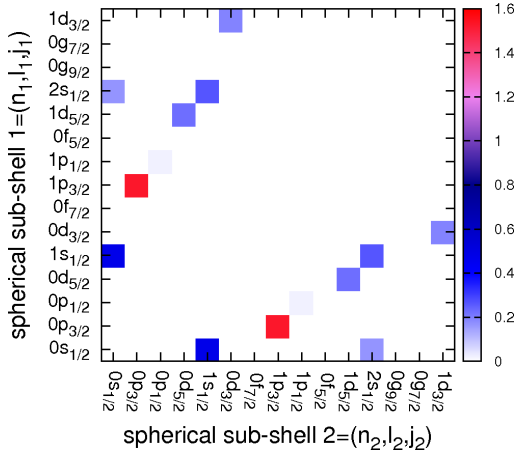

NUMERICAL ALGORITHM WITH ORBITAL OPTIMIZATION

Evolution of the one-body density: Representation of $\Delta\rho=|\rho_{HF}-\rho_{correlated}|$ in HF basis

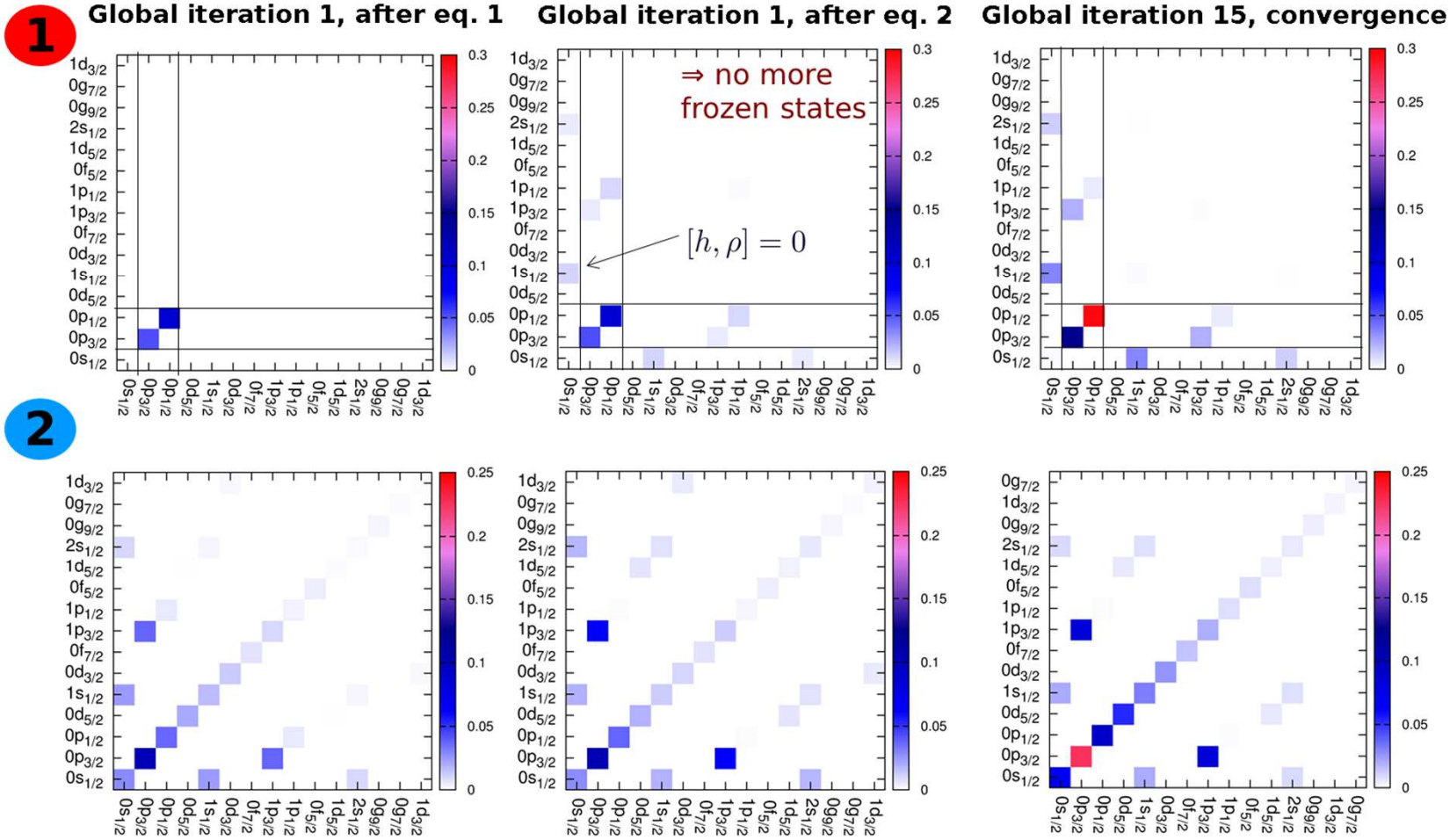

NUMERICAL ALGORITHM WITH ORBITAL OPTIMIZATION

Convergence of the one-body density matrix

Iteration 1

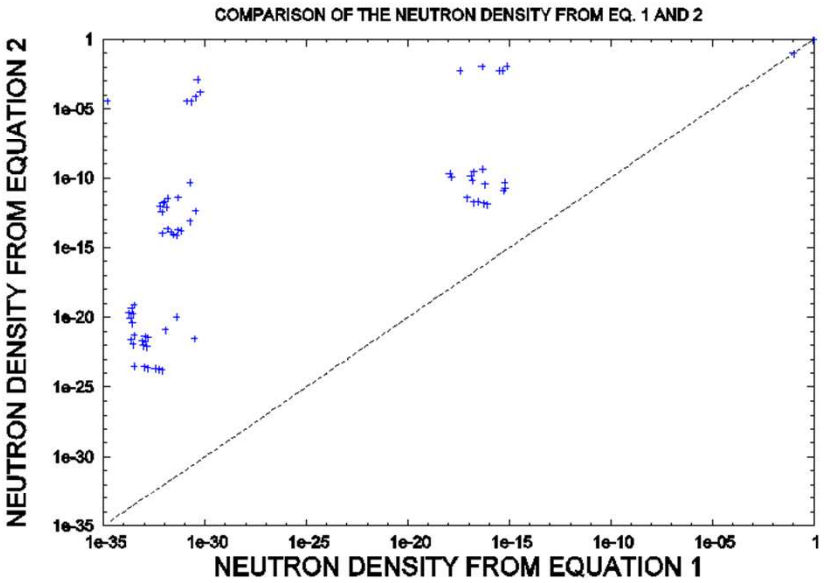

1

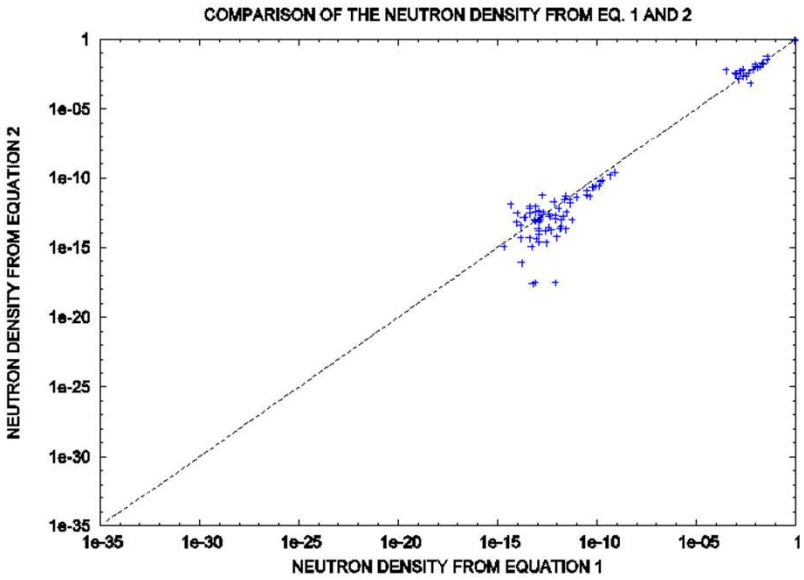

2

NUMERICAL ALGORITHM WITH ORBITAL OPTIMIZATION

Iteration 2

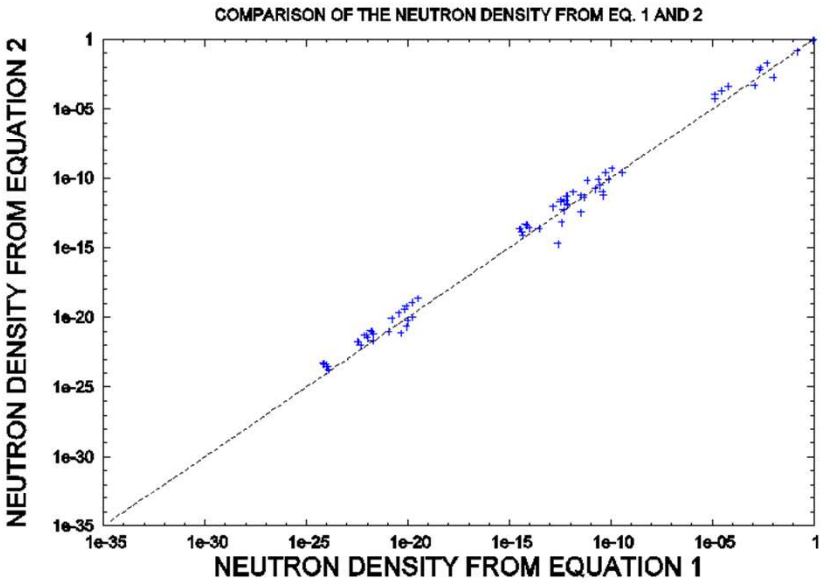

1

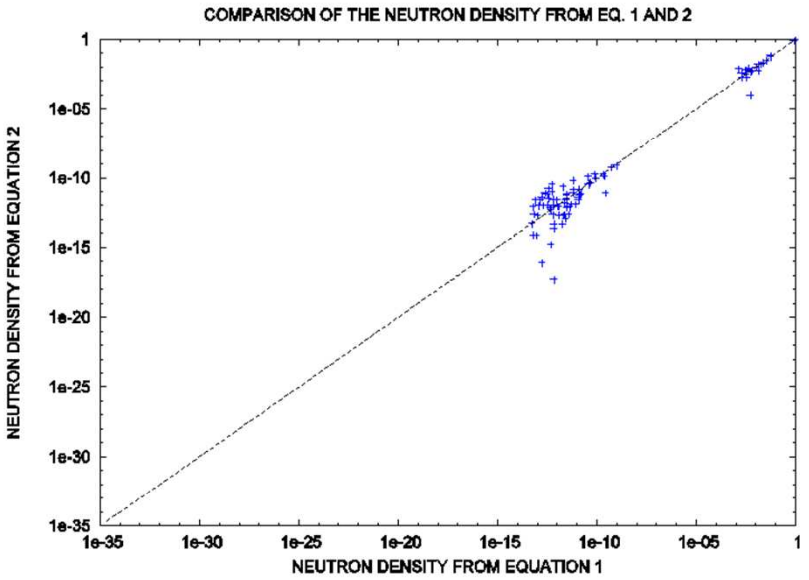

2

NUMERICAL ALGORITHM WITH ORBITAL OPTIMIZATION

Iteration 3

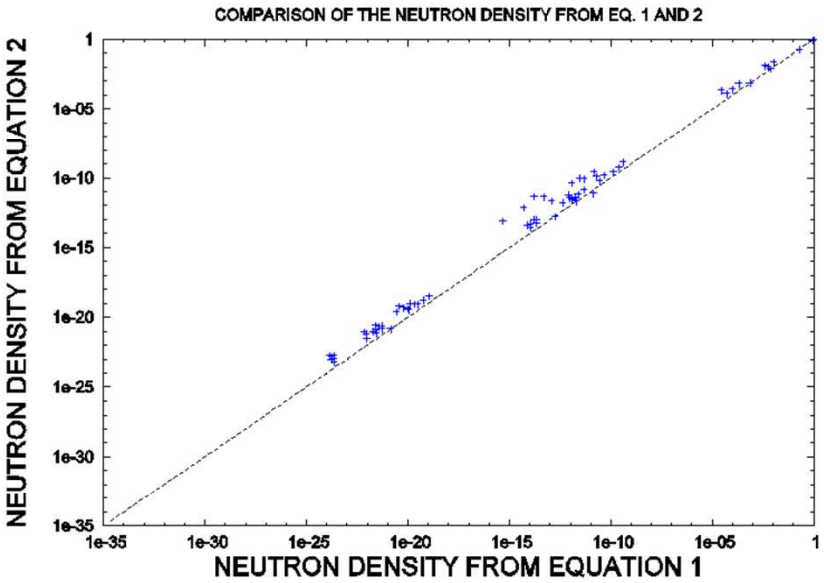

1

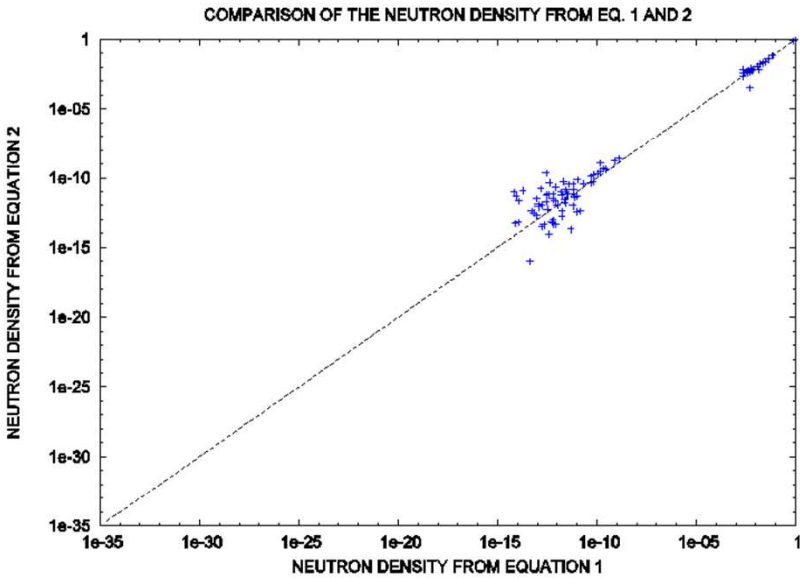

2

NUMERICAL ALGORITHM WITH ORBITAL OPTIMIZATION

Iteration 4

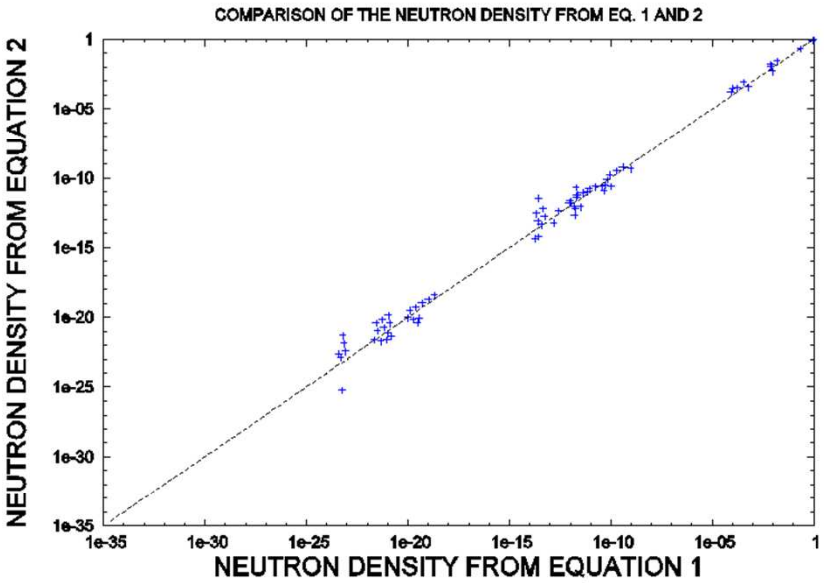

1

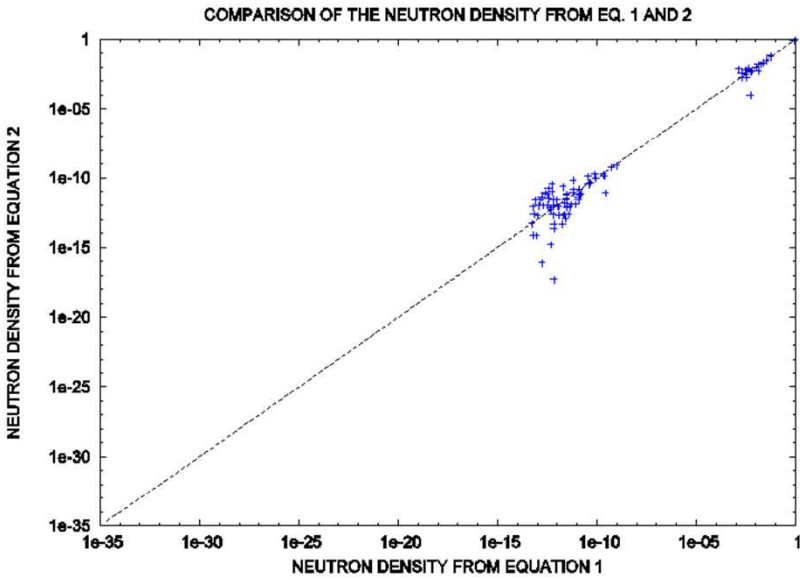

2

NUMERICAL ALGORITHM WITH ORBITAL OPTIMIZATION

Iteration 5

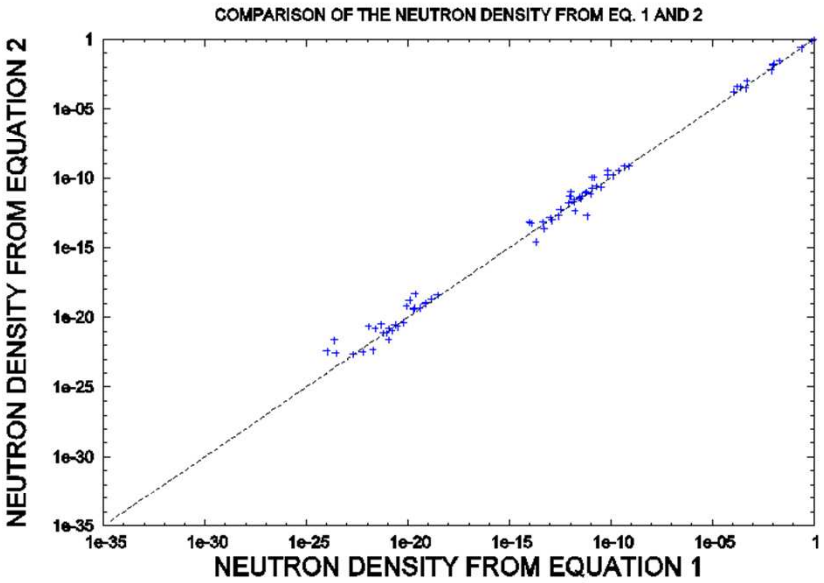

1

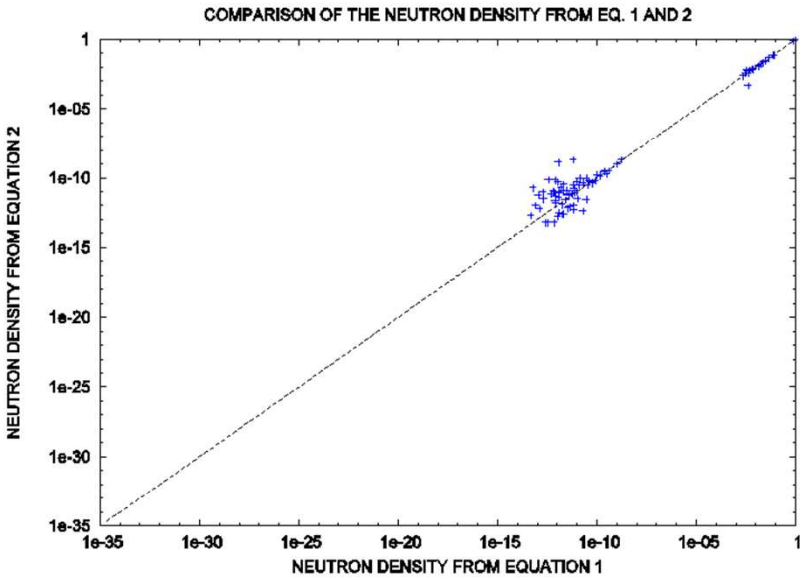

2

NUMERICAL ALGORITHM WITH ORBITAL OPTIMIZATION

Iteration 6

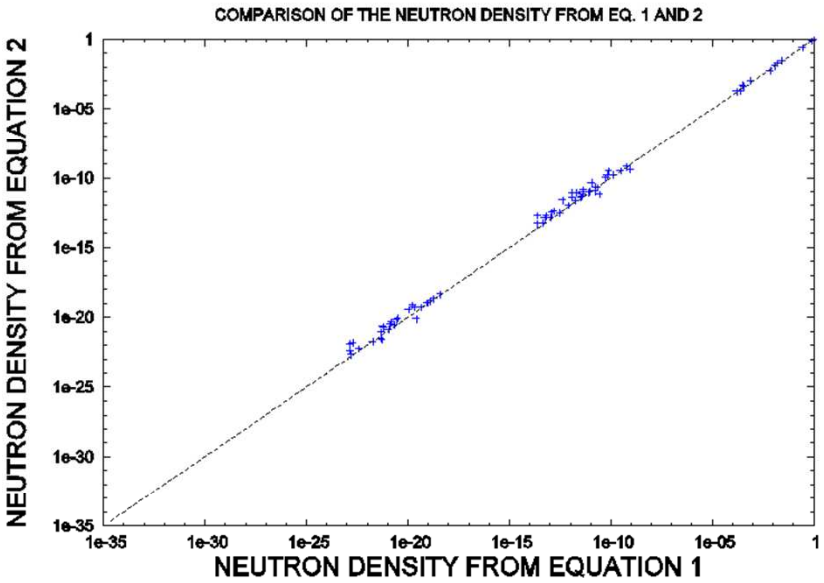

1

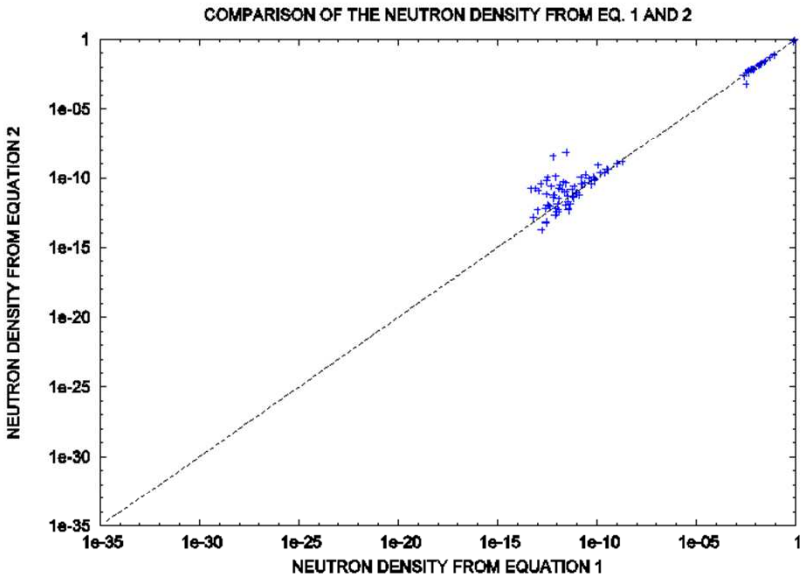

2

NUMERICAL ALGORITHM WITH ORBITAL OPTIMIZATION

Iteration 7

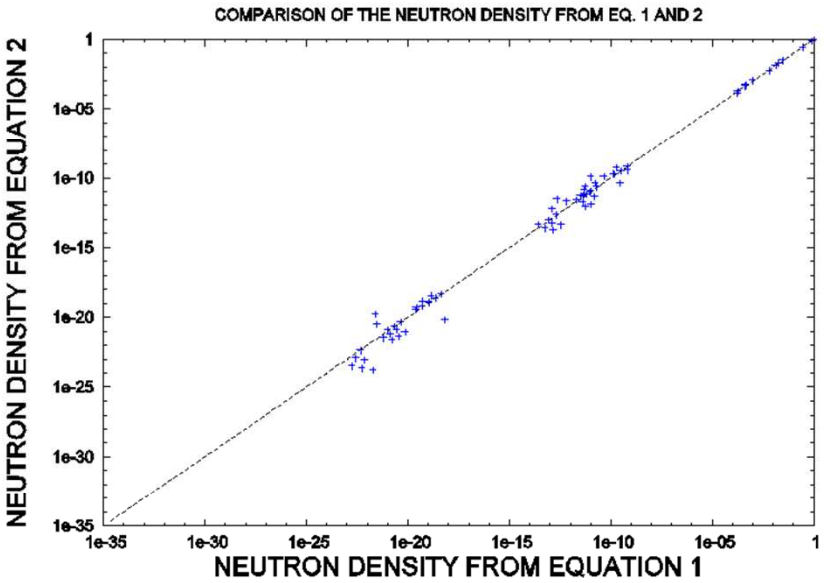

1

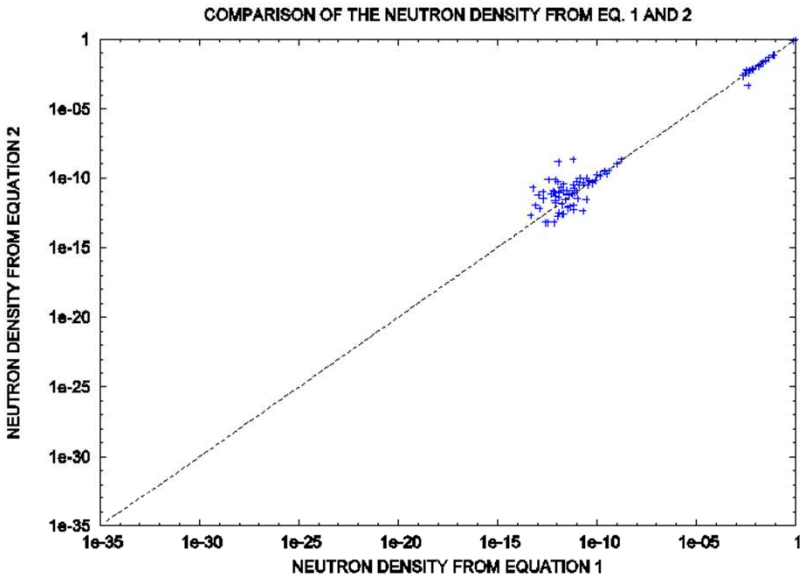

2

NUMERICAL ALGORITHM WITH ORBITAL OPTIMIZATION

Iteration 8

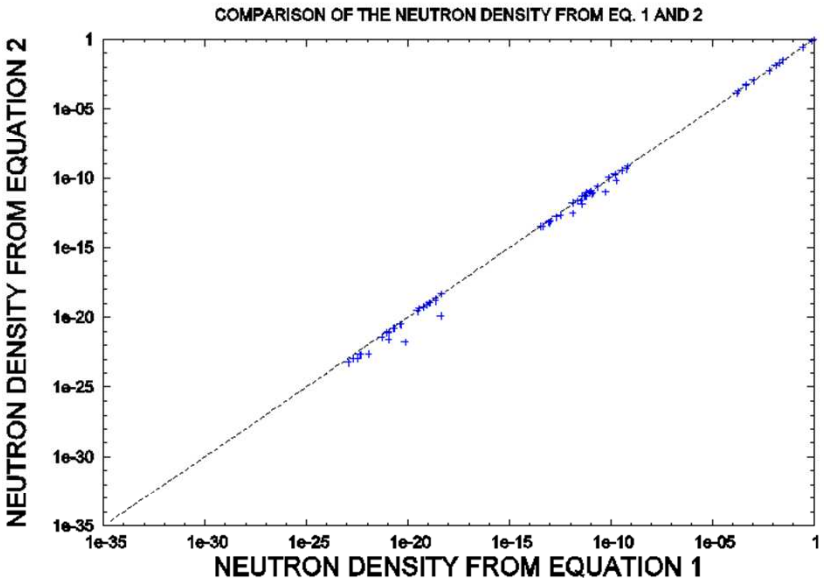

1

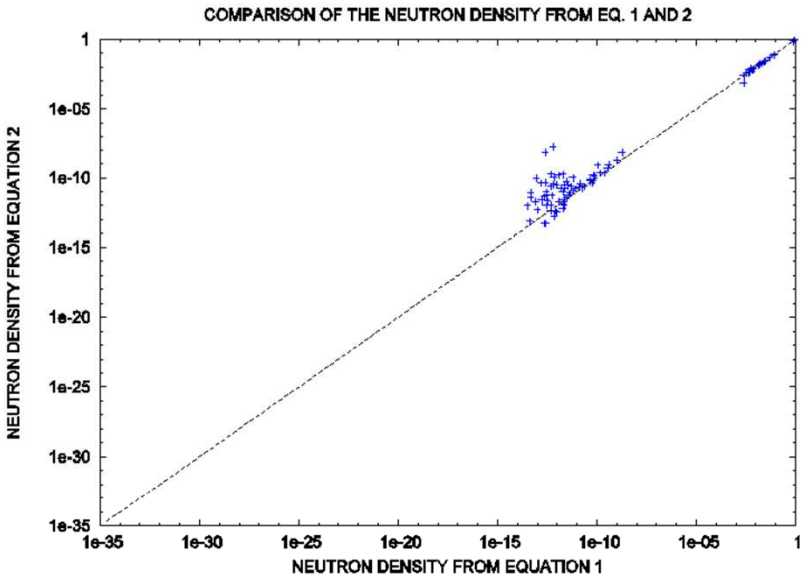

2

NUMERICAL ALGORITHM WITH ORBITAL OPTIMIZATION

Iteration 9

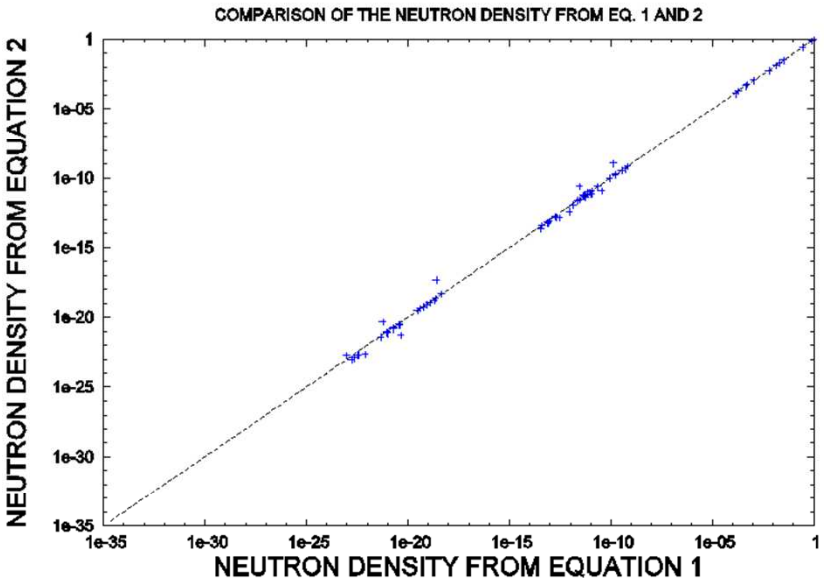

1

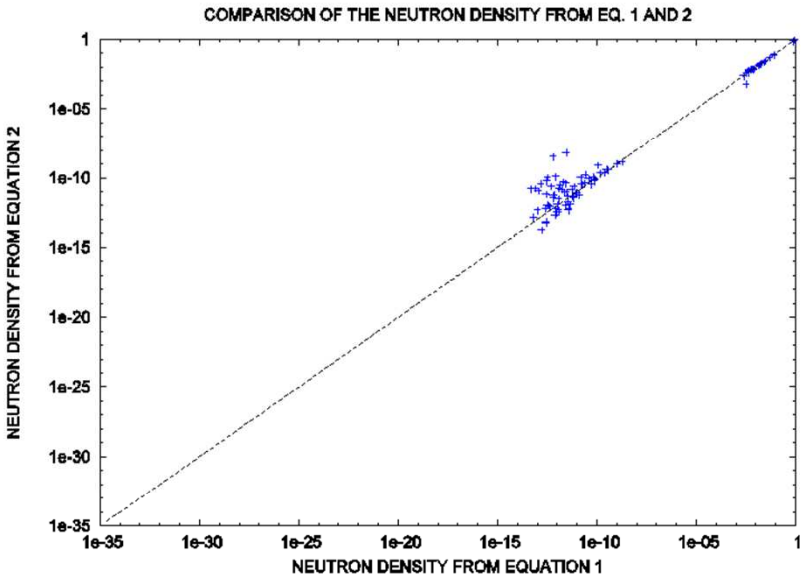

2

NUMERICAL ALGORITHM WITH ORBITAL OPTIMIZATION

Iteration 10

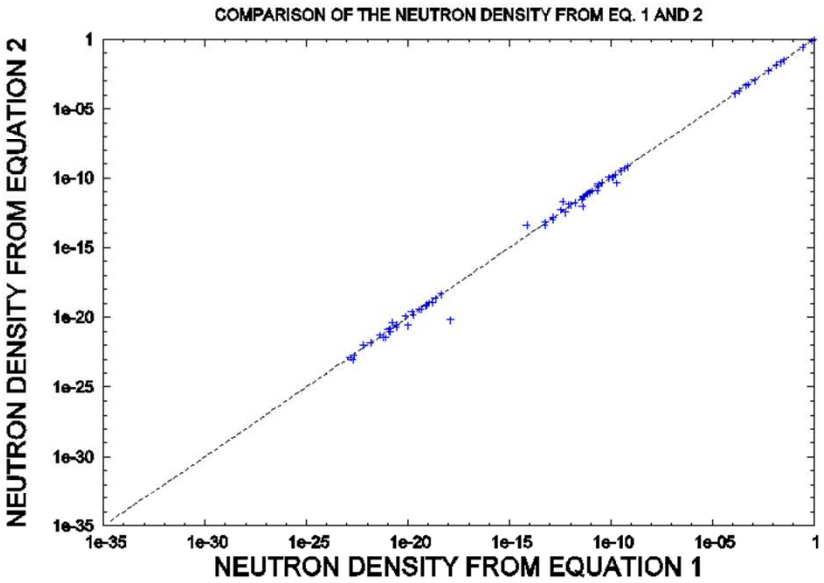

1

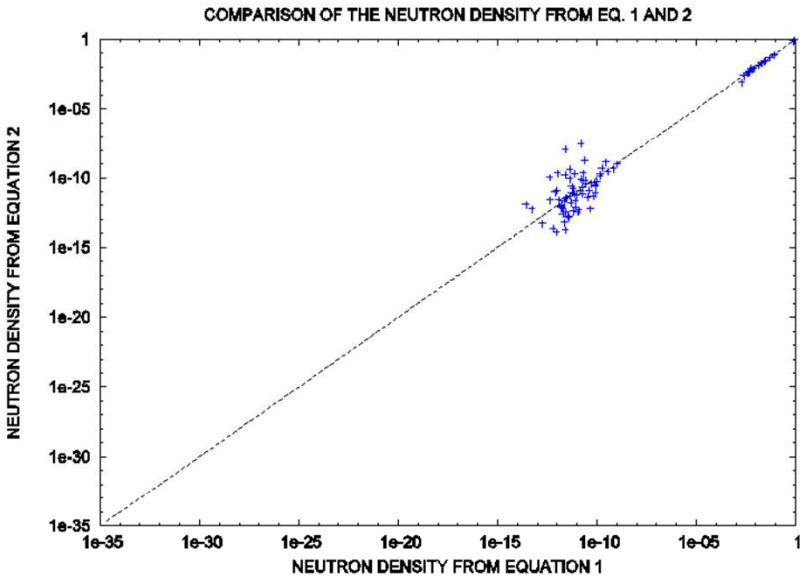

2

NUMERICAL ALGORITHM WITH ORBITAL OPTIMIZATION

Iteration 12

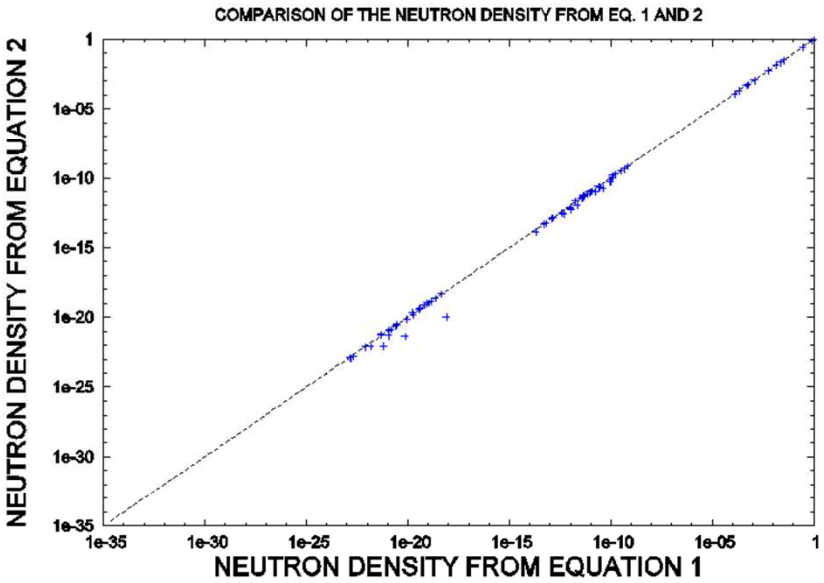

1

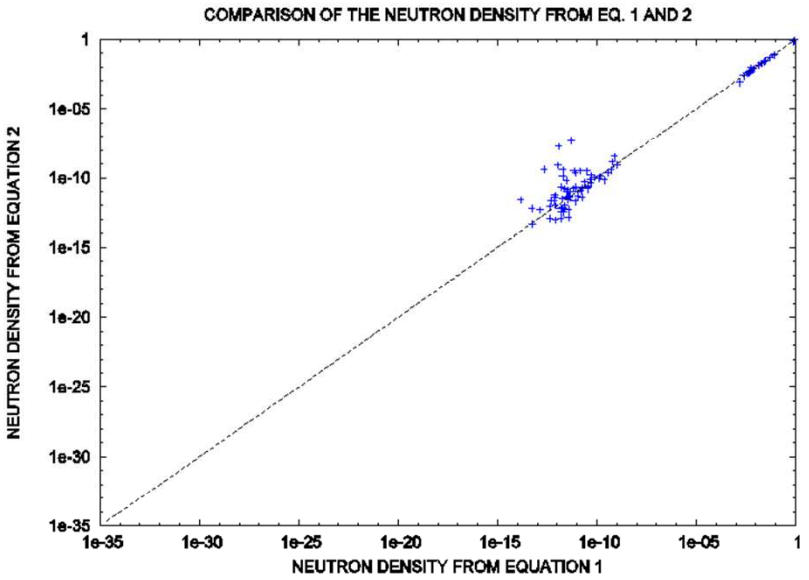

2

NUMERICAL ALGORITHM WITH ORBITAL OPTIMIZATION

Iteration 13

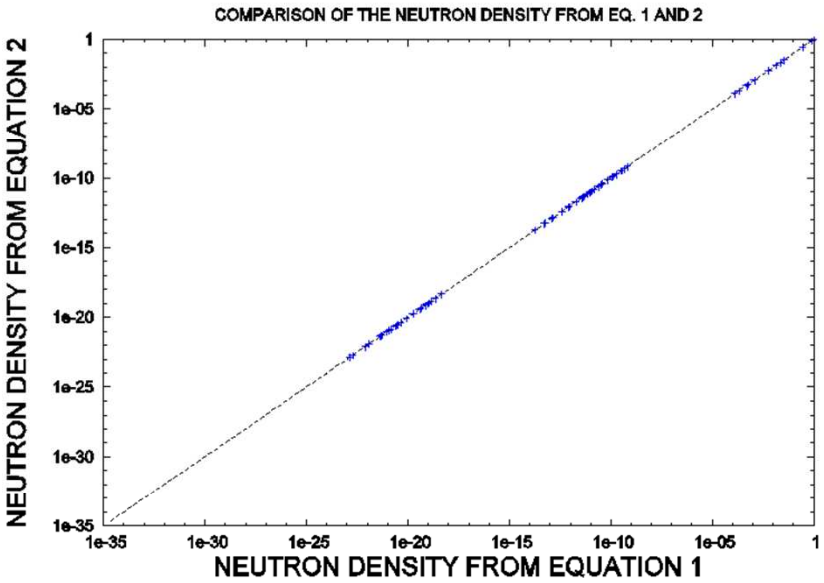

1

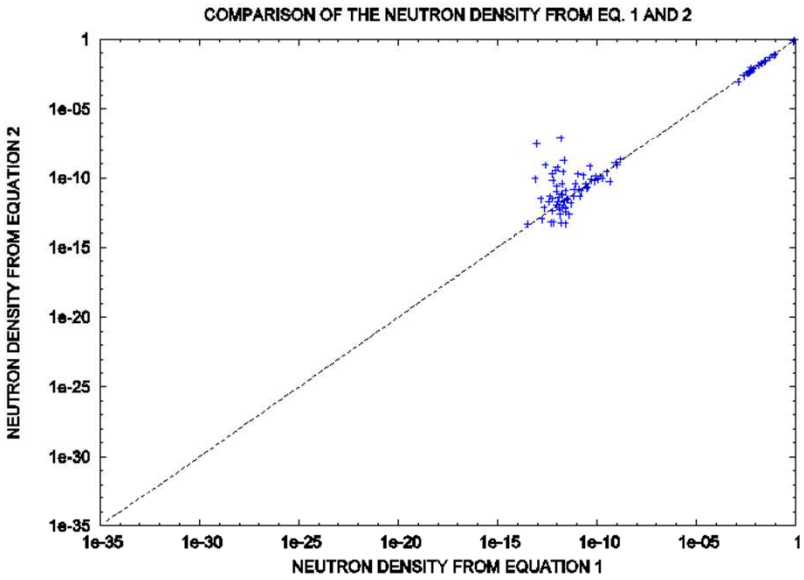

2

NUMERICAL ALGORITHM WITH ORBITAL OPTIMIZATION

Iteration 14

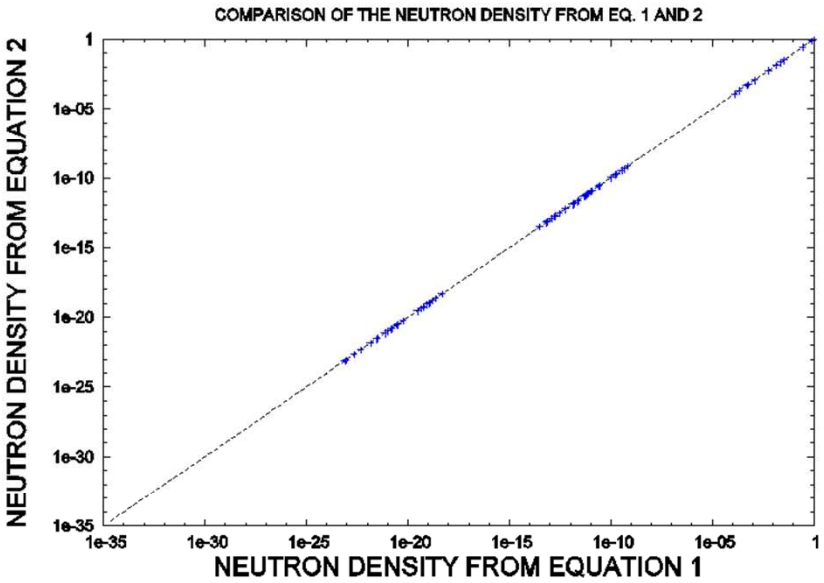

1

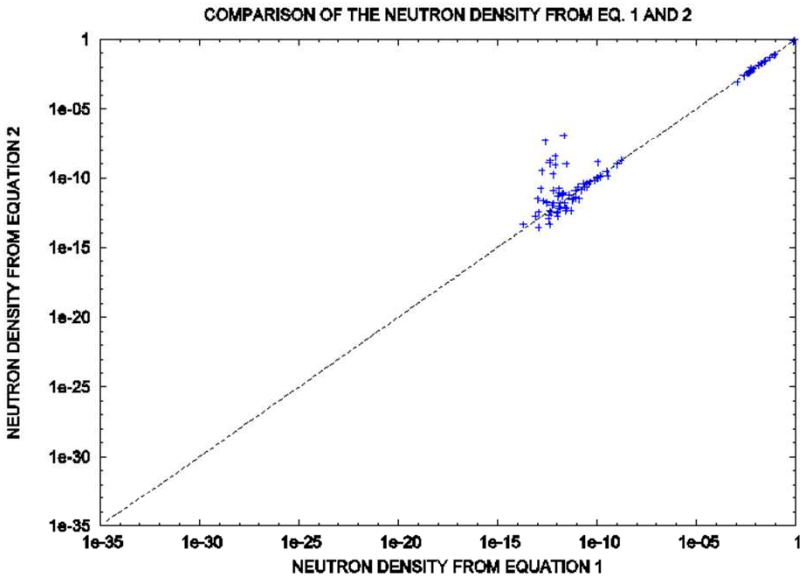

2

NUMERICAL ALGORITHM WITH ORBITAL OPTIMIZATION

Iteration 15

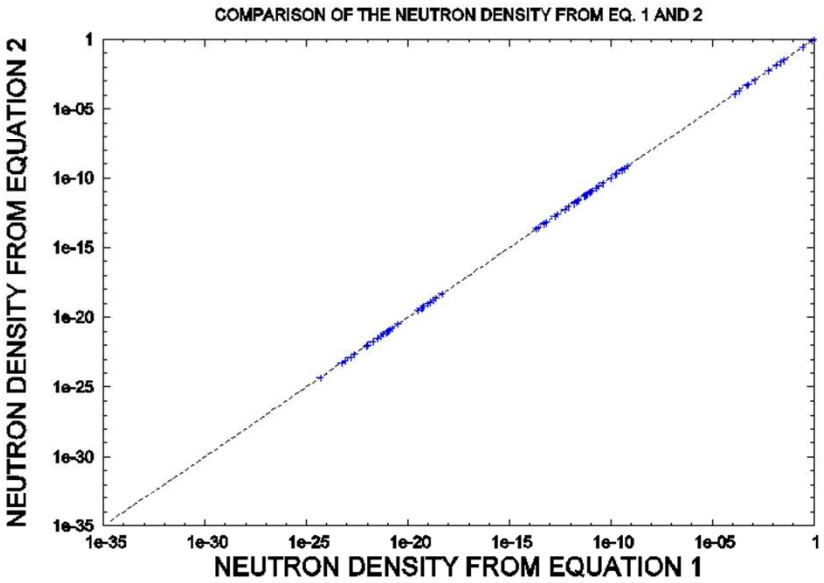

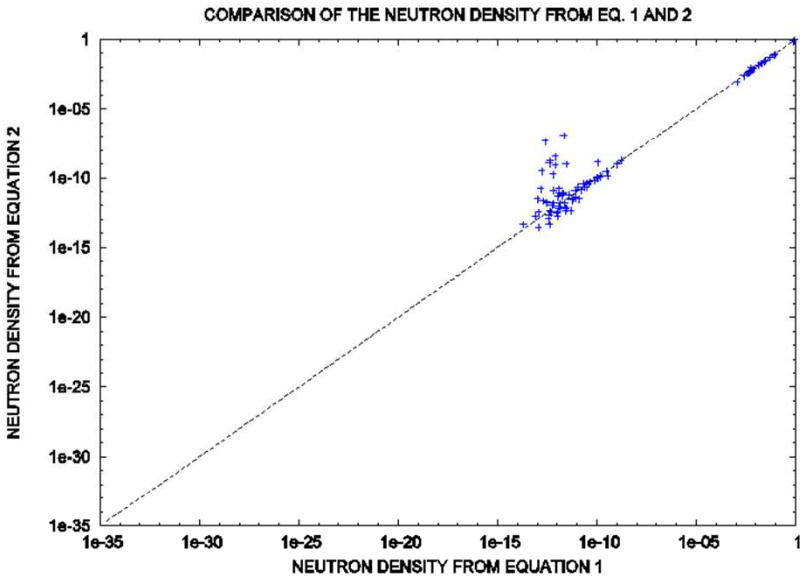

1

2

NUMERICAL ALGORITHM WITH ORBITAL OPTIMIZATION

Iteration 15

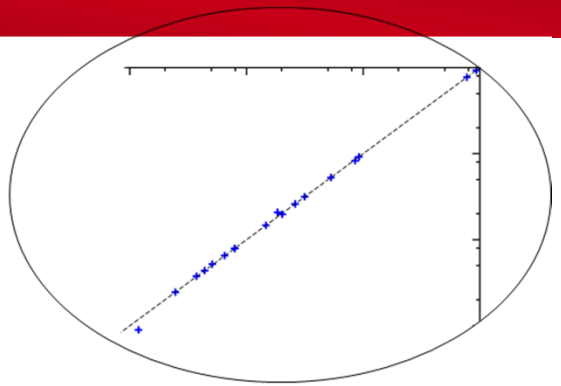

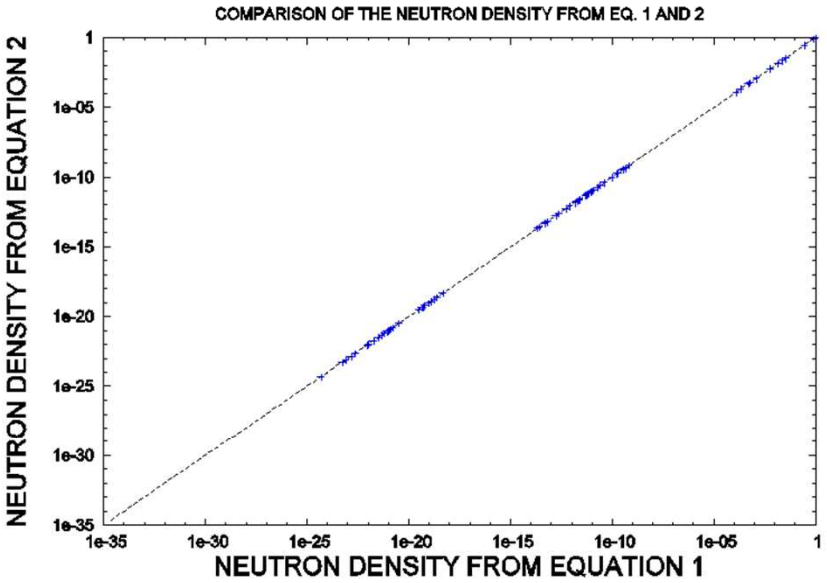

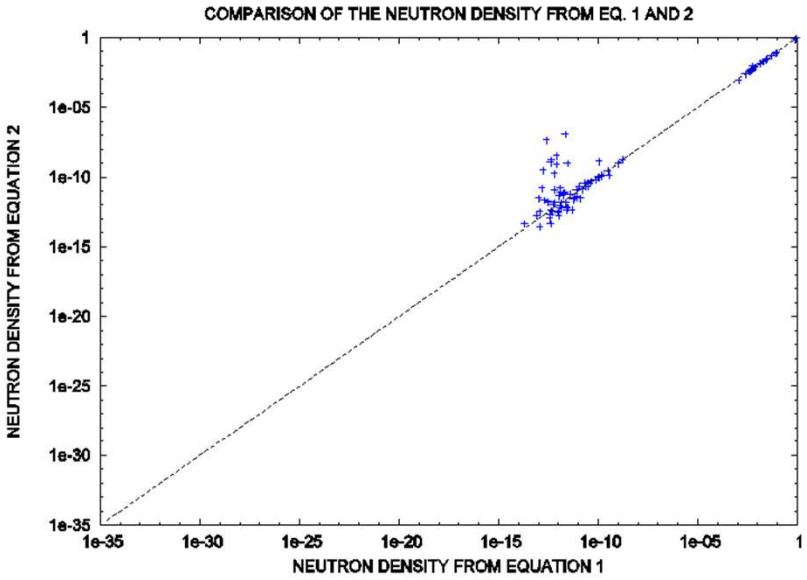

1

2

NUMERICAL ALGORITHM WITH ORBITAL OPTIMIZATION

1

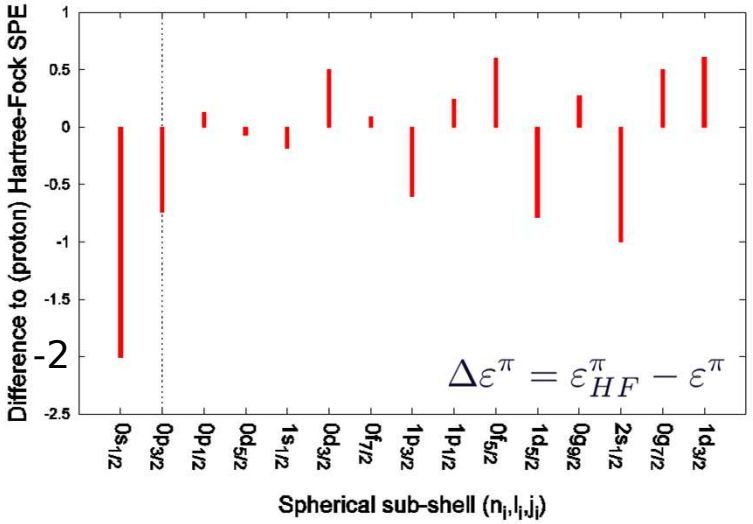

2

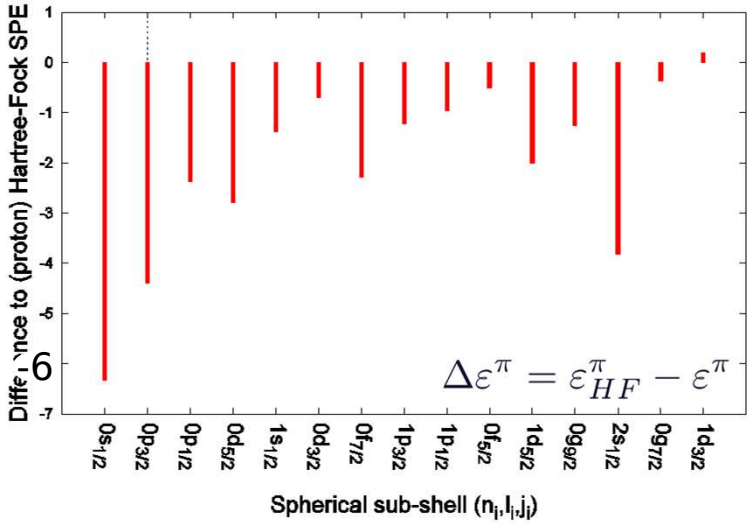

Modifications of the single-particle energies

Eigenvalues ε of $h[\rho,\sigma]_{ij} = T_{ij} + \sum_{kl}\langle ik|\widetilde{V}|jl\rangle\rho_{lk} + \frac{1}{4}\sum_{klmn}\langle kl|\frac{\partial\widetilde{V}}{\partial\rho_{ji}}|mn\rangle\langle\Psi|a^{\dagger}_{k}a^{\dagger}_{l}a_{n}a_{m}|\Psi\rangle$ compared to ε_{HF}.

1

- Spectrum compressed by ~2.5 MeV
- 0s increased by ~2 MeV
- Gap $0p_{3/2}$-$0p_{1/2}$ (8.15 MeV) reduced by ~870 keV.

2

- Spectrum compressed by ~6 MeV
- 0s increased by ~6 MeV
- Gap $0p_{3/2}$-$0p_{1/2}$ (8.15 MeV) reduced by ~2 MeV.

NUMERICAL ALGORITHM WITH ORBITAL OPTIMIZATION

1

Correlation energy E_{corr} (MeV)	
1^{st} equation	$1^{st}+2^{nd}$ equation
6.22	6.56

2

Correlation energy E_{corr} (MeV)	
1^{st} equation	$1^{st}+2^{nd}$ equation
61.77	62.54

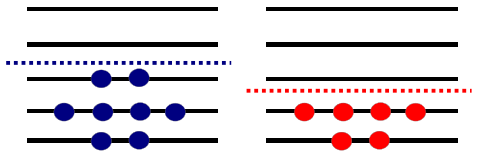

Effect on the ground state

- HF binding energy: E(HF)= -92.9 MeV
- Experimental binding energy: E(HF)= -92.16 MeV

- Correlation energy: $E_{corr} = E(\Psi) - E(HF)$ (correlated state: Ψ; Hartree-Fock state: HF)

1

Gain 340 keV

2

Gain 770 keV

- Clear overbinding in ^{12}C!
- What is happening with the interaction, related to the truncation scheme?

NUMERICAL ALGORITHM WITH ORBITAL OPTIMIZATION

Effect on the ground state

- **0P0H component**

	1^{st} equation only (HF orbitals)	$1^{st} + 2^{nd}$ equations (HF orbitals)	$1^{st} + 2^{nd}$ equations (SC orbitals)
0p-0h	53.95	47.65	48.20

0p-0h	21.46	20.39	22.33

- **Weight of $\mathcal{Q}^{(i)}$ in the final state $|\Psi^{(f)}\rangle$**

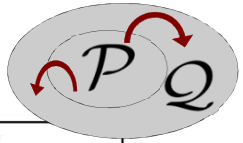

	1^{st} equation only		$1^{st} + 2^{nd}$ equations	
valence	weight of $\mathcal{P}^{(i)}$	weight of $\mathcal{Q}^{(i)}$	weight of $\mathcal{P}^{(i)}$	weight of $\mathcal{Q}^{(i)}$
0p-shell	100 %	0 %	98.87 %	**1.13** %
0s-0p	100 %	0 %	97.42 %	**2.58** %
0s-0p-1s0d	100 %	0 %	96.93 %	**4.13** %
0s-0p-1s0d-0f1p	100 %	0 %	95.87 96.93%	**3.07**%
...	...	...	...	...

$$\mathcal{P}^{(f)} = 98.87\%\,\mathcal{P}^{(i)} + 1.13\%\,\mathcal{Q}^{(i)}$$

⟹ **Need to find balance between explicit configurations and effect of orbital equation**

NUMERICAL ALGORITHM WITH ORBITAL OPTIMIZATION

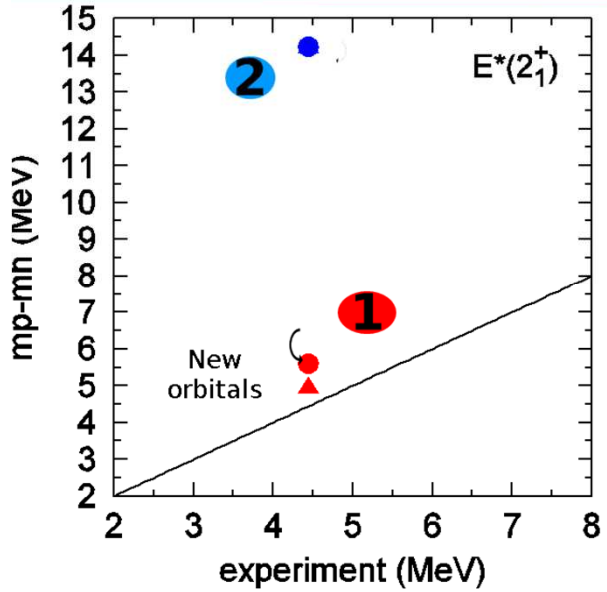

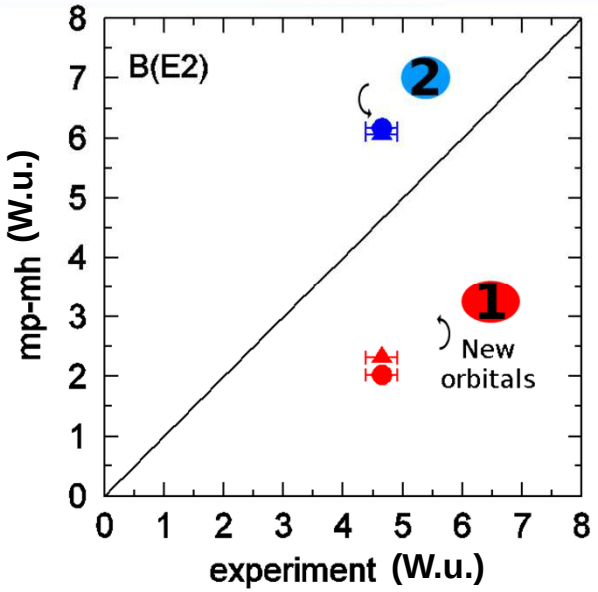

Study of the first 2+ excited state

1 0ħω space

- Precise description of energy
- Lack of collectivity

2 Nħω space

- bad description of energy
- collectivity much improved

⇒ **Systematic improvement of results by orbital equation**
⇒ **Need to find optimal truncation scheme**
⇒ **Interaction ?**

SELF-CONSISTENT MULTIPARTICLE-MULTIHOLE CONFIGURATION MIXING

I. General overview
- ✓ General context
- ✓ Link with Green's functions: Exact solution
- ✓ Optimization of orbitals: Truncated solution

II. Numerical algorithm with orbital optimization
- ✓ ^{12}C test nucleus

III. Various applications with the Gogny force
- ✓ Structure: sd-shell nuclei
- ✓ Reactions: (e,e') and (p,p') inelastic scattering

IV. Work in progress
- ✓ Derivation of an effective interaction
- ✓ Complex scaling
- ✓ Fitting of a generalized Gogny interaction
- ✓ Effective operators

VARIOUS APPLICATIONS WITH THE GOGNY FORCE

PHYSICAL REVIEW C **78**, 024305 (2008)

Variational multiparticle-multihole configuration mixing method applied to pairing correlations in nuclei

N. Pillet,[1] J.-F. Berger,[1] and E. Caurier[2]

[1]*CEA, DPTA, Service de Physique Nucléaire, Bruyères-le-Châtel, F-91297 Arpajon, France*
[2]*Département Recherches Subatomiques, Institut Pluridisciplinaire Hubert Curien, 23 rue du Loess, BP28, F-67037 Strasbourg, France*

(Received 16 June 2008; published 12 August 2008)

Applying a variational multiparticle-multihole configuration mixing method whose purpose is to include correlations beyond the mean field in a unified way without particle number and Pauli principle violations, we investigate pairing-like correlations in the ground states of ^{116}Sn, ^{106}Sn, and ^{100}Sn. The same effective nucleon-nucleon interaction, namely, the D1S parametrization of the Gogny force, is used to derive both the mean field and correlation components of nuclear wave functions. Calculations are performed using an axially symmetric representation. The structure of correlated wave functions, their convergence with respect to the number of particle-hole excitations, and the influence of correlations on single-particle level spectra and occupation probabilities are analyzed and compared with results obtained with the same two-body effective interaction from BCS, Hartree-Fock-Bogoliubov, and particle
nuclear radii and the first theoretical excited
projected after variation BCS approaches. Calculations of
experimental data.

PHYSICAL REVIEW C **85**, 044315 (2012)

Low-lying spectroscopy of a few even-even silicon isotopes investigated with the multiparticle-multihole Gogny energy density functional

N. Pillet,[1] V. G. Zelevinsky,[2] M. Dupuis,[1] J.-F. Berger,[1] and J. M. Daugas[1]

[1]*CEA, DAM, DIF, F-91297 Arpajon, France*
sics and Astronomy and National Superconducting Cyclotron Laboratory, Michigan State University,
East Lansing, Michigan 48824, USA

October 2011; revised manuscript received 29 December 2011; published 16 April 2012)

tion microscopic method has been applied with the Gogny effective interaction to the
ng positive-parity states in even-even $^{26-32}$Si isotopes. The aim of the study is to compare the
h with those of a standard method of generator coordinate method (GCM) type and to get
ve power of multiconfiguration methods employed with effective nucleon-nucleon force
culations. It is found that the multiconfiguration approach leads to an excellent description
opy of ^{26}Si, ^{28}Si, and ^{32}Si, but gives a systematic energy shift in ^{30}Si. A careful analysis
that this discrepancy originates from too large proton-neutron matrix elements supplied
the level of the approximate resolution of the multiparticle-multihole configuration
present study. These proton-neutron matrix elements enter in the definition of both
s and coupling matrix elements. Finally, a statistical analysis of highly excited
med, revealing exponential convergence in agreement with previous work in the
ach. This latter result provides strong
d an implicit treatment of

PHYSICAL REVIEW C **89**, 011306(R) (2014)

First characterization of *sd*-shell nuclei with a multiconfiguration approach

J. Le Bloas,[1] N. Pillet,[1] M. Dupuis,[1] J. M. Daugas,[1] L. M. Robledo,[2] C. Robin,[1] and V. G. Zelevinsky[3]

[1]*CEA, DAM, DIF, F-91297 Arpajon, France*
[2]*Universitad autonoma de Madrid, Madrid, Spain*
[3]*Department of Physics and Astronomy and National Superconducting Cyclotron Laboratory, Michigan State University, East Lansing, Michigan 48824, USA*

(Received 1 August 2013; published 30 January 2014)

In this work, we propose a new description of nuclear spectroscopy based on the analysis of a rather complete set of observables, using the multiparticle-multihole configuration mixing and the D1S Gogny interaction. The application to the even-even *sd*-shell nuclei, for both ground and 0_2^+, 1_1^+, 2_1^+, 2_2^+, 3_1^+, 3_2^+, 4_1^+ excited states, clearly shows the pertinence of this approach. The standard deviation to experiment is ~500 keV for two-nucleon separation energies and ~400 keV for excitation energies. The calculated magnetic dipole moments and $B(M1)$ transition probabilities are in a very good agreement with experiment. Concerning the spectroscopic quadrupole moments and $B(E2)$ transition probabilities, the experimental trends are systematically reproduced. Only a lack of quadrupole collectivity appears. A solution to improve this expected defect is suggested.

VARIOUS APPLICATIONS WITH THE GOGNY FORCE

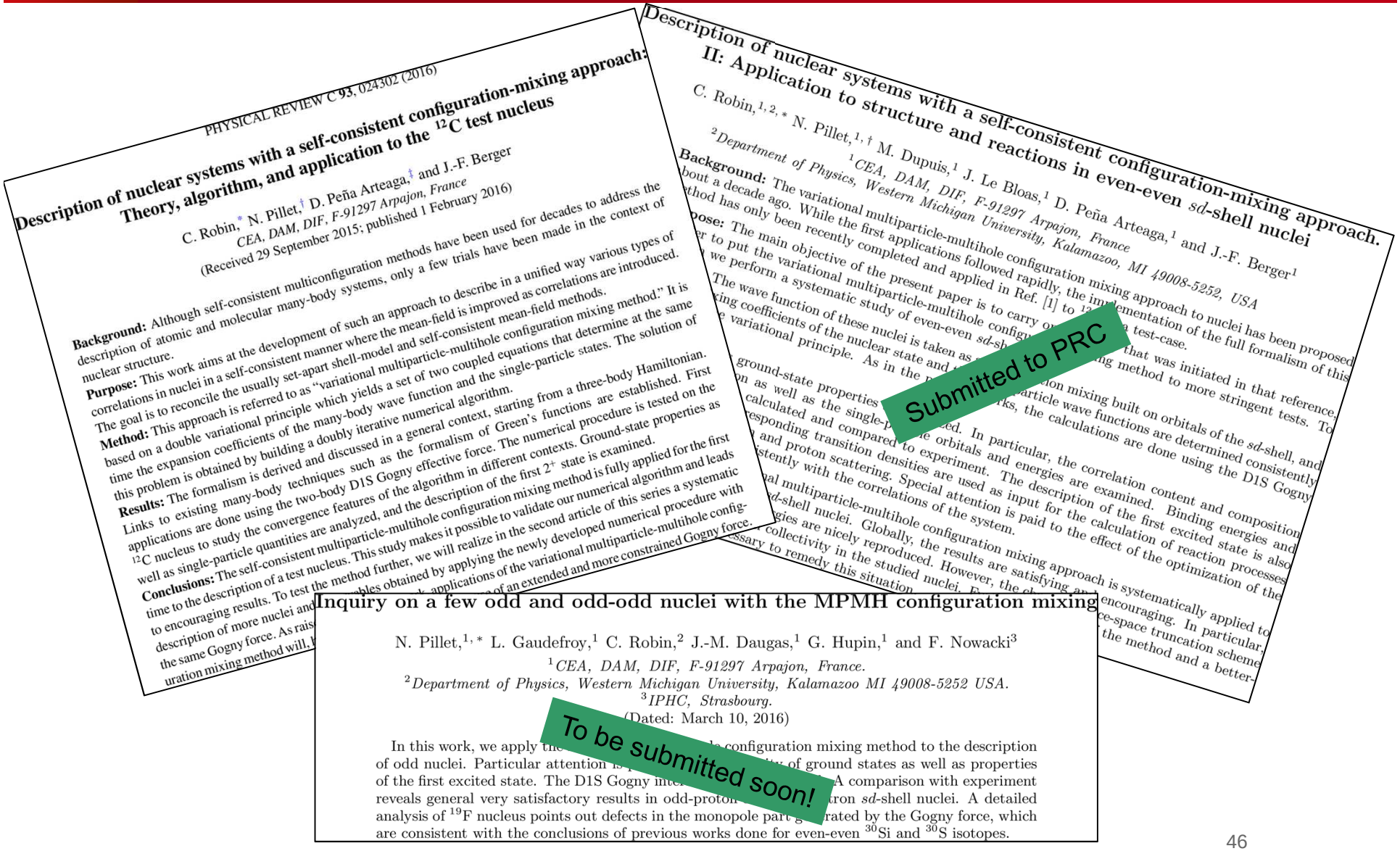

PHYSICAL REVIEW C 93, 024302 (2016)

Description of nuclear systems with a self-consistent configuration-mixing approach: Theory, algorithm, and application to the ^{12}C test nucleus

C. Robin,* N. Pillet,† D. Peña Arteaga,‡ and J.-F. Berger

CEA, DAM, DIF, F-91297 Arpajon, France

(Received 29 September 2015; published 1 February 2016)

Background: Although self-consistent multiconfiguration methods have been used for decades to address the description of atomic and molecular many-body systems, only a few trials have been made in the context of nuclear structure.

Purpose: This work aims at the development of such an approach to describe in a unified way various types of correlations in nuclei in a self-consistent manner where the mean-field is improved as correlations are introduced. The goal is to reconcile the usually set-apart shell-model and self-consistent mean-field methods.

Method: This approach is referred to as "variational multiparticle-multihole configuration mixing method." It is based on a double variational principle which yields a set of two coupled equations that determine at the same time the expansion coefficients of the many-body wave function and the single-particle states. The solution of this problem is obtained by building a doubly iterative numerical algorithm.

Results: The formalism is derived and discussed in a general context, starting from a three-body Hamiltonian. Links to existing many-body techniques such as the formalism of Green's functions are established. First applications are done using the two-body D1S Gogny effective force. The numerical procedure is tested on the well as single-particle quantities are analyzed, and the description of the first 2^+ state is examined. Ground-state properties as ^{12}C nucleus to study the convergence features of the algorithm in different contexts. Ground-state properties as time to the description of a test nucleus. This study makes it possible to validate our numerical algorithm and leads to encouraging results. To test the method further, we will realize in the second article of this series a systematic description of more nuclei and

Conclusions: The self-consistent multiparticle-multihole configuration mixing method is fully applied for the first the same Gogny force. As rais

Description of nuclear systems with a self-consistent configuration-mixing approach. II: Application to structure and reactions in even-even *sd*-shell nuclei

C. Robin, N. Pillet, M. Dupuis, J. Le Bloas, D. Peña Arteaga, and J.-F. Berger

Department of Physics, Western Michigan University, Kalamazoo, MI 49008-5252, USA

CEA, DAM, DIF, F-91297 Arpajon, France

Submitted to PRC

Inquiry on a few odd and odd-odd nuclei with the MPMH configuration mixing

N. Pillet, L. Gaudefroy, C. Robin, J.-M. Daugas, G. Hupin, and F. Nowacki

CEA, DAM, DIF, F-91297 Arpajon, France.

Department of Physics, Western Michigan University, Kalamazoo MI 49008-5252 USA.

IPHC, Strasbourg.

(Dated: March 10, 2016)

To be submitted soon!

VARIOUS APPLICATIONS WITH THE GOGNY FORCE

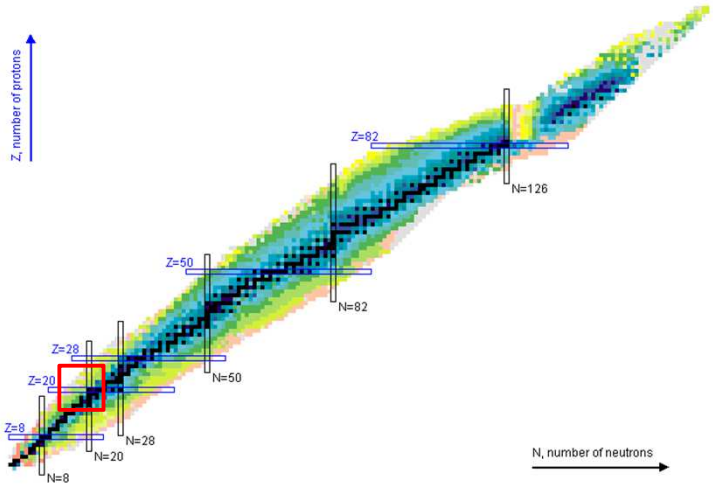

Framework:

- Even-even nuclei $10 \leq (Z,N) \leq 18$
- Truncation scheme: core of ^{16}O (non frozen) + valence

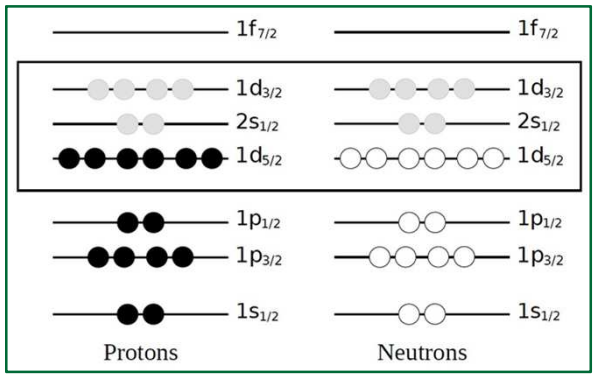

Ex: $^{28}Si \rightarrow$ 12P12H

- N_0=9 major oscillator shells

Description of ground state and spectroscopic properties

- Binding and separation energies, charge radii
- Excitation energies
- Magnetic dipole moments μ and quadrupole spectroscopic moments Q_s
- Transition probabilities B(E2) and B(M1)
- Inelastic electron and proton scattering on discrete states

⟹ How are these observables affected by the optimization of orbitals?

VARIOUS APPLICATIONS WITH THE GOGNY FORCE

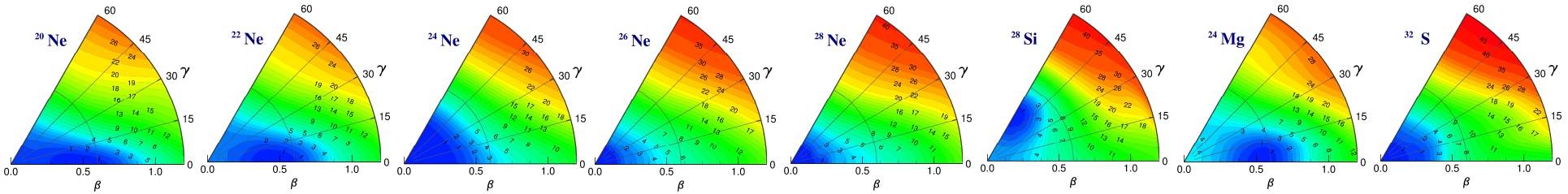

MPMH configuration mixing calculations done at 3 levels:

- Level 1

Without any self-consistency, i.e. after one single diagonalization of the many-body matrix $H(\rho_{HF}) = T + V^{D1S}(\rho_{HF})$ in the sd-shell of pure Hartree-Fock (HF) orbitals

- Level 2

With partial self-consistency, i.e. after solving the full 1st equation alone, on HF orbitals, including the correlated density in the interaction and the rearrangement terms. This is achieved by diagonalizing iteratively, until convergence. In this work, convergence is said to be reached when the difference between any element of the one-body density matrix between two iterations $N-1$ and N is less than 10^{-5}.

- Level 3

With full self-consistency, i.e. when both equations are solved together and consistency between correlations and orbitals is reached. This is achieved using the doubly-iterative procedure described previously. The convergence criteria on the density matrix is also set to 10^{-5} for both types of iterations.

VARIOUS APPLICATIONS WITH THE GOGNY FORCE

Ground state properties

- **Binding energy**

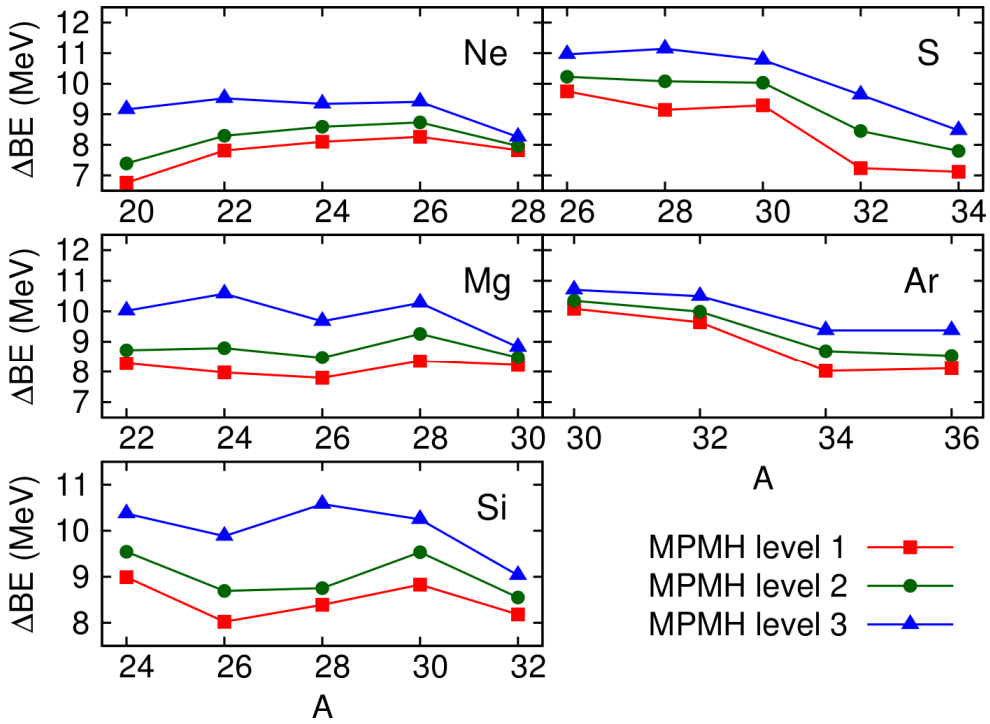

Average difference
- Level 1: 8.91 MeV
- Level 3: 9.84 MeV

Standard deviation
- Level 1: 0.793 MeV
- Level 3: 0.789 MeV

- **Correlation energy**

	Level 1: Eq. (2) with $\rho = \rho_{HF}$, $\sigma = 0$.	Level 2: Full Eq. (2).	Level 3: Full Eqs. (2)& (3).
^{28}Ne	1.15	1.28	1.58
^{26}Ne	0.41	0.88	1.55
^{24}Ne	5.75	6.23	6.98
^{22}Ne	10.48	10.90	12.12
^{20}Ne	10.93	11.54	13.30
^{24}Mg	14.24	15.06	16.04
^{28}Si	5.89	6.25	8.08
^{32}S	3.37	4.58	5.76

VARIOUS APPLICATIONS WITH THE GOGNY FORCE

- **0P0H components in the ground states**

Nucleus	Configuration	Level 1: Eq. (2) with $\rho = \rho_{HF}$, $\sigma = 0$. (HF orbitals)	Level 2: Full Eq. (2). (HF orbitals)	Level 3: Full Eqs. (2)& (3). (SC orbitals)	Level 3: Full Eqs. (2)& (3). (HF orbitals)
^{28}Ne	**0p-0h**	**86.24**	**84.11**	**83.63**	
	$(1p\text{-}1h)_\pi$ $(0d_{5/2} \to 1s)$	3.49	3.19	2.85	
	$(1p\text{-}1h)_\nu$ $(1s \to 0d_{3/2})$	3.26	4.04	4.50	
^{26}Ne	**0p-0h**	**77.11**	**70.88**	**69.62**	**61.50**
	$(1p\text{-}1h)_\nu$ $(1s \to 0d_{3/2})$	6.02	7.28	7.59	
	$(1p\text{-}1h)_\nu$ $(0d_{5/2} \to 0d_{3/2})$	4.45	4.87	5.20	
	$(2p\text{-}2h)_{\pi\nu}$ $(1s^\nu \otimes 0d^\pi_{5/2} \to 0d^\nu_{3/2} \otimes 1s^\pi)$	2.27	2.75	2.38	
^{24}Ne	**0p-0h**	**56.51**	**53.45**	**49.41**	
	$(1p\text{-}1h)_\nu$ $(0d_{5/2} \to 1s)$	17.81	17.48	17.81	
	$(1p\text{-}1h)_\nu$ $(0d_{5/2} \to 0d_{3/2})$	5.60	6.27	6.34	
	$(2p\text{-}2h)_\nu$ $(0d_{5/2} \to 1s)$	6.17	6.56	7.54	
^{20}Ne	**0p-0h**	**45.36**	**43.05**	**33.05**	
	$(2p\text{-}2h)_{\pi\nu}$ $(0d^\pi_{5/2} \otimes 0d^\nu_{5/2} \to 1s^\pi \otimes 1s^\nu)$	8.15	6.80	8.86	
	$(1p\text{-}1h)_\pi$ $(0d_{5/2} \to 0d_{3/2})$	6.91	8.26	8.65	
	$(1p\text{-}1h)_\nu$ $(0d_{5/2} \to 0d_{3/2})$	6.94	8.30	8.58	
	$(1p\text{-}1h)_\pi$ $(0d_{5/2} \to 1s)$	5.29	4.44	5.08	
	$(1p\text{-}1h)_\nu$ $(0d_{5/2} \to 1s)$	5.40	4.50	5.13	
	$(2p\text{-}2h)_\pi$ $(0d_{5/2} \otimes 0d_{5/2} \to 1s \otimes 1s)$	2.32	1.89	2.46	
	$(2p\text{-}2h)_\nu$ $(0d_{5/2} \otimes 0d_{5/2} \to 1s \otimes 1s)$	2.44	1.95	2.52	
^{24}Mg	**0p-0h**	**34.63**	**32.45**	**23.82**	
	$(1p\text{-}1h)_\nu$ $(0d_{5/2} \to 1s)$	8.31	7.13	6.49	
	$(1p\text{-}1h)_\pi$ $(0d_{5/2} \to 1s)$	8.08	6.98	6.37	
	$(2p\text{-}2h)_{\pi\nu}$ $(0d^\pi_{5/2} \otimes 0d^\nu_{5/2} \to 1s^\pi \otimes 1s^\nu)$	5.30	4.32	5.16	
	$(1p\text{-}1h)_\nu$ $(0d_{5/2} \to 0d_{3/2})$	4.43	4.83	3.94	
	$(1p\text{-}1h)_\pi$ $(0d_{5/2} \to 0d_{3/2})$	4.37	4.83	3.96	
	$(2p\text{-}2h)_\nu$ $(0d_{5/2} \otimes 0d_{5/2} \to 1s \otimes 1s)$	2.24	1.83	2.26	
	$(2p\text{-}2h)_\pi$ $(0d_{5/2} \otimes 0d_{5/2} \to 1s \otimes 1s)$	2.12	1.76	2.17	
^{28}Si	**0p-0h**	**26.02**	**38.68**	**17.80**	**16.99**
	$(2p\text{-}2h)_{\pi\nu}$ $(0d^\pi_{5/2} \otimes 0d^\nu_{5/2} \to 1s^\pi \otimes 1s^\nu)$	12.36	8.11	8.98	
	$(2p\text{-}2h)_\nu$ $(0d_{5/2} \otimes 0d_{5/2} \to 1s \otimes 1s)$	5.03	3.28	3.66	
	$(2p\text{-}2h)_\pi$ $(0d_{5/2} \otimes 0d_{5/2} \to 1s \otimes 1s)$	4.87	3.17	3.54	
^{32}S	**0p-0h**	**60.30**	**47.23**	**26.20**	**24.26**
	$(2p\text{-}2h)_{\pi\nu}$ $(1s^\pi \otimes 1s^\nu \to 0d^\pi_{3/2} \otimes 0d^\nu_{3/2})$	8.36	9.31	11.20	
	$(2p\text{-}2h)_\nu$ $(1s \otimes 1s \to 0d_{3/2} \otimes 0d_{3/2})$	3.80	4.38	5.47	
	$(2p\text{-}2h)_\pi$ $(1s \otimes 1s \to 0d_{3/2} \otimes 0d_{3/2})$	4.11	4.80	5.87	

VARIOUS APPLICATIONS WITH THE GOGNY FORCE

- **Single-particle states – Energies/Spectrum**

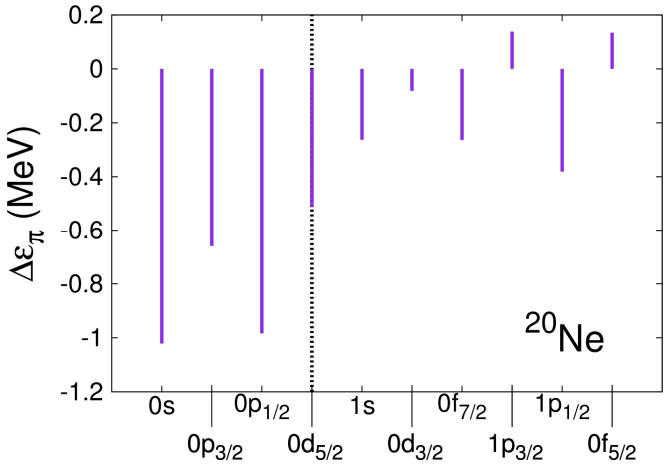

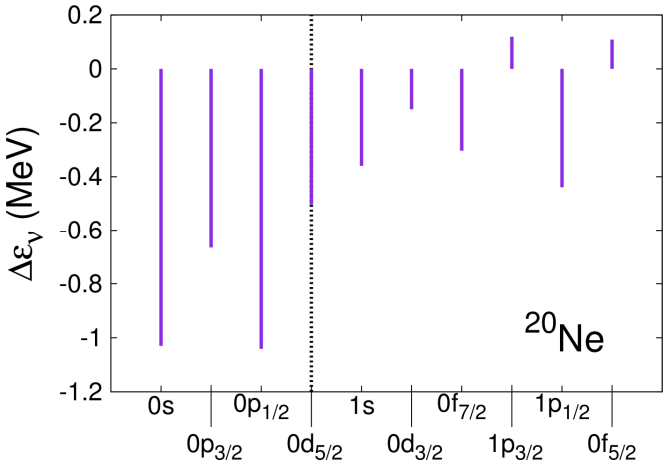

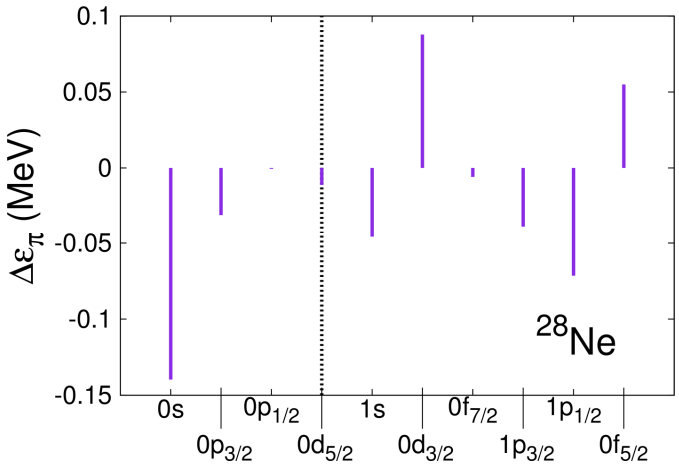

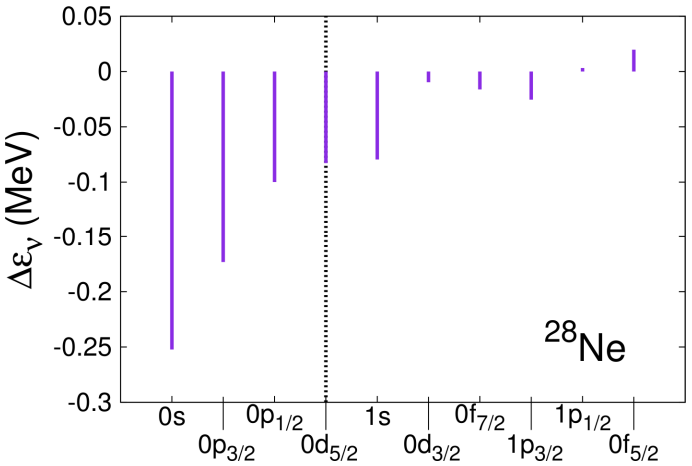

VARIOUS APPLICATIONS WITH THE GOGNY FORCE

- **Single-particle states – Radial part**

^{20}Ne

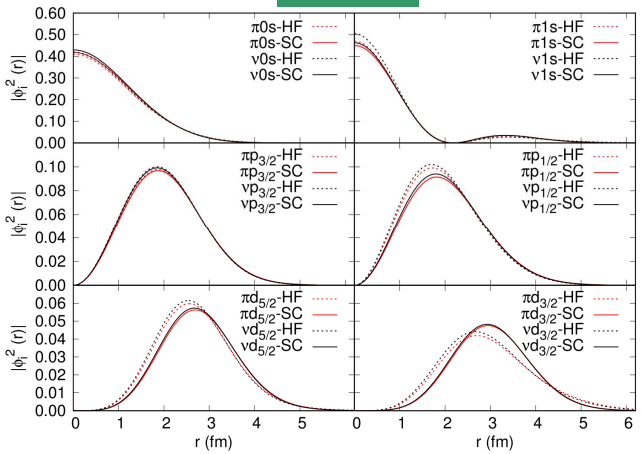

^{28}Ne

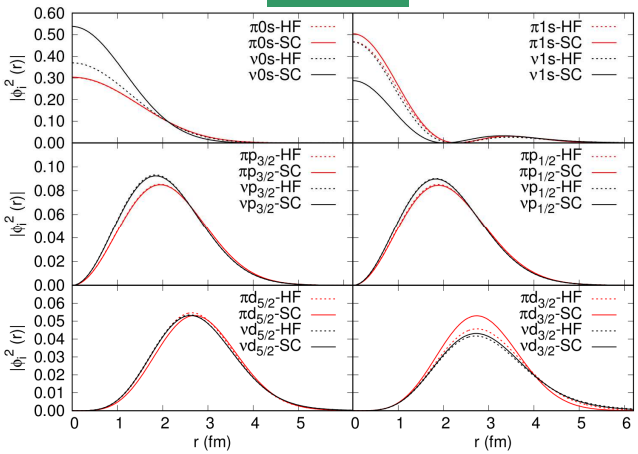

^{24}Mg

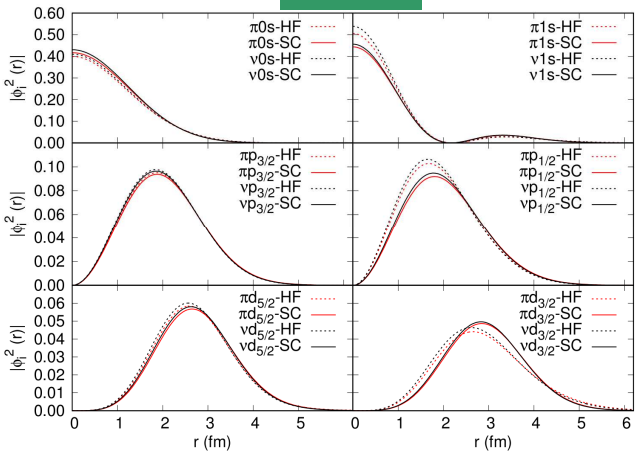

^{28}Si

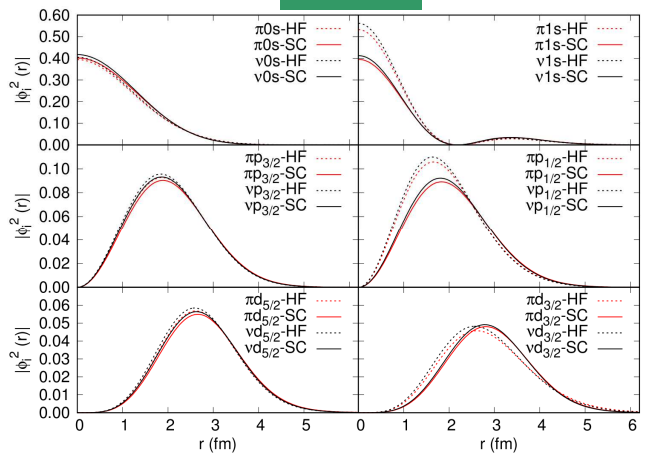

^{32}S

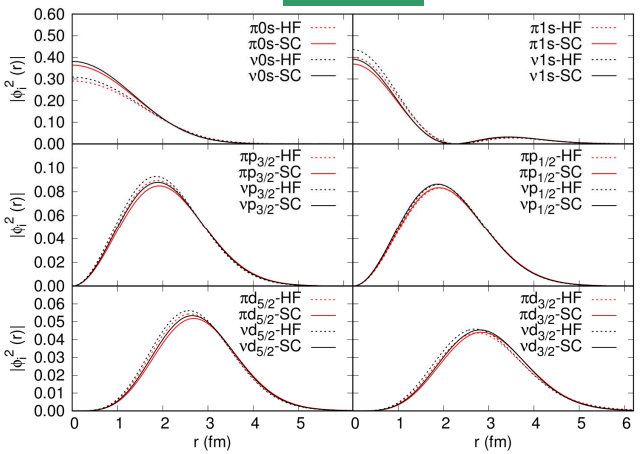

VARIOUS APPLICATIONS WITH THE GOGNY FORCE

- **Charge radii**

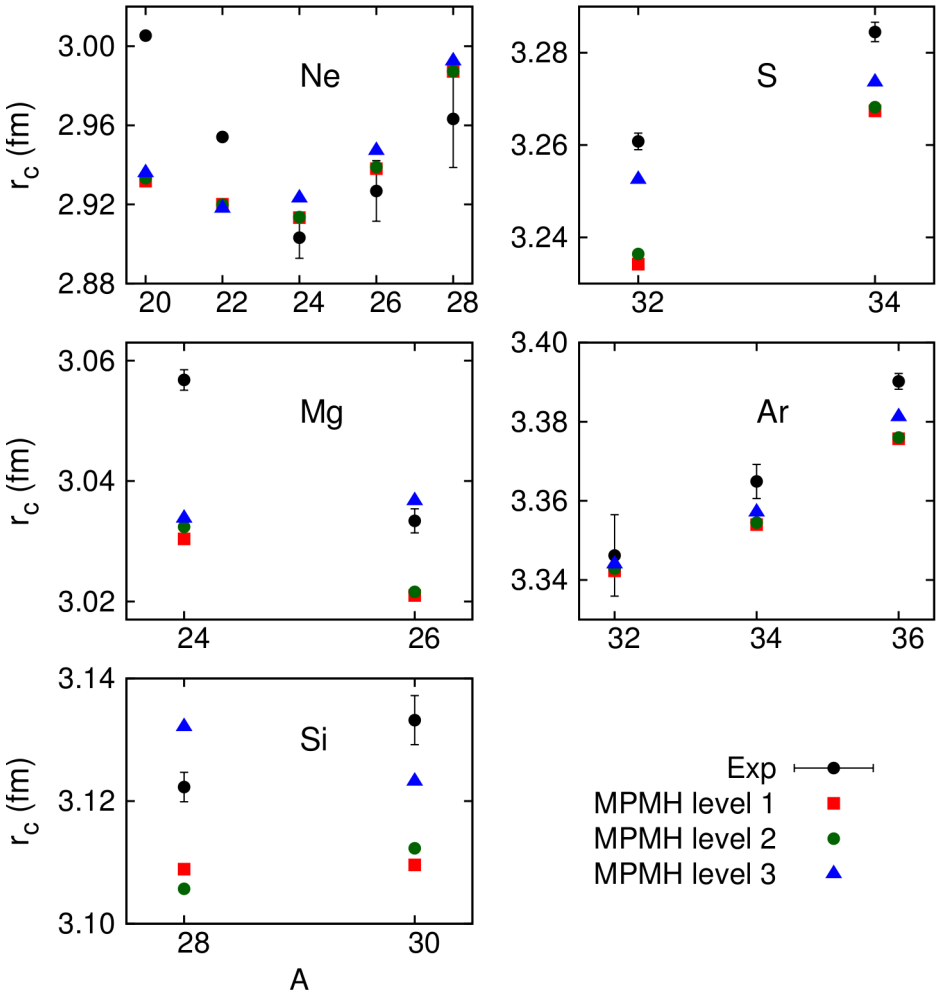

Average difference
- Level 1: 0.021 fm
- Level 3: 0.018 fm

Standard deviation
- Level 1: 0.017 fm
- Level 3: 0.018 fm

VARIOUS APPLICATIONS WITH THE GOGNY FORCE

- **Radial proton and neutron densities**

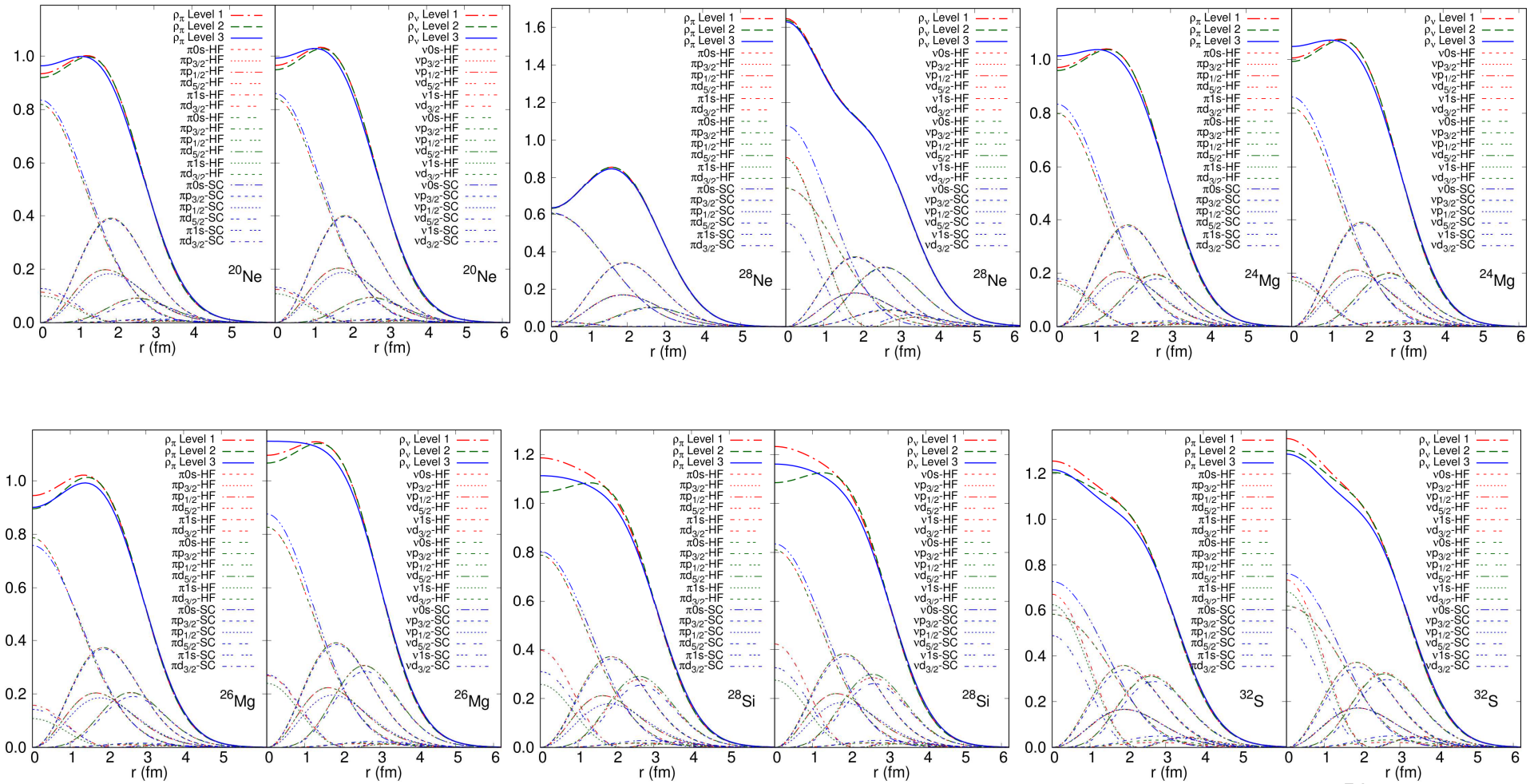

VARIOUS APPLICATIONS WITH THE GOGNY FORCE

First 2^+ excited state and B(E2) transition probabilities toward the ground state

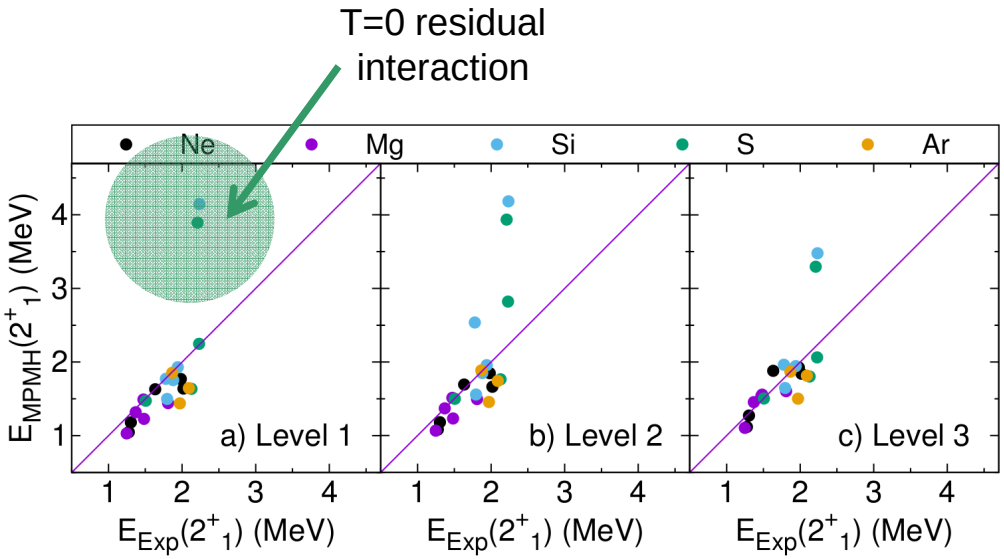

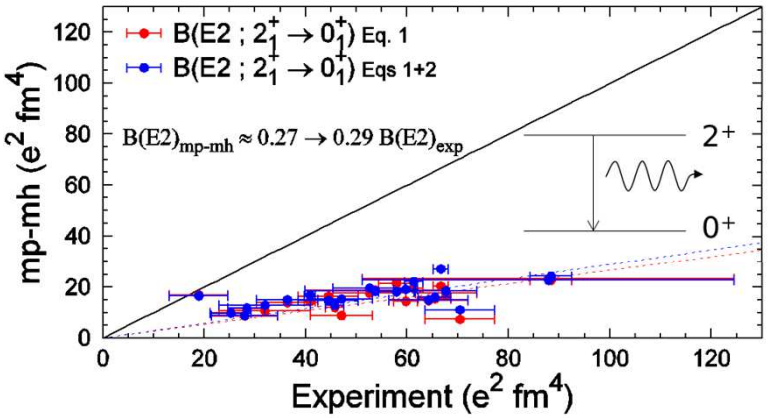

Average difference
- Level 1: 373 keV
- Level 3: 235 keV

Standard deviation
- Level 1: 517 keV
- Level 3: 323 keV

Excluding ^{30}Si and ^{30}S

Average difference
- Level 1: 226 keV
- Level 3: 142 keV

Standard deviation
- Level 1: 214 keV
- Level 3: 122 keV

- Experimental trends globally well reproduced but...
- Clear lack of collectivity due to the restricted valence space
- Little but positive effect from optimization of orbitals

VARIOUS APPLICATIONS WITH THE GOGNY FORCE

Inelastic electron scattering between discrete states: Form factor

$$F_\lambda(q) = \frac{\sqrt{4\pi}}{Z}\sqrt{\frac{2J_f+1}{2J_i+1}}\int_0^\infty r^2\,dr\; j_\lambda(qr)\,\rho_{tr}(r)$$

From MPMH:

$$\rho^{nn'}_{\alpha\alpha'} = \langle\psi_{n'}|a^\dagger_{\alpha'}a_\alpha|\psi_n\rangle$$

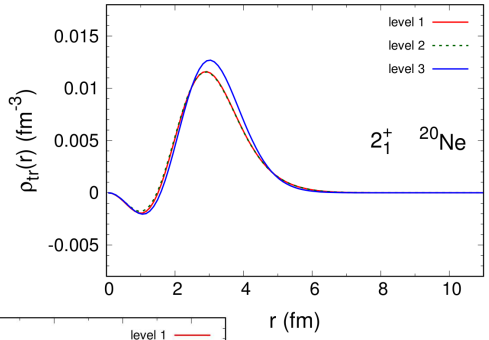

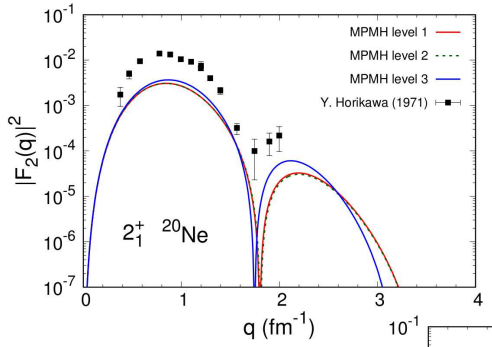

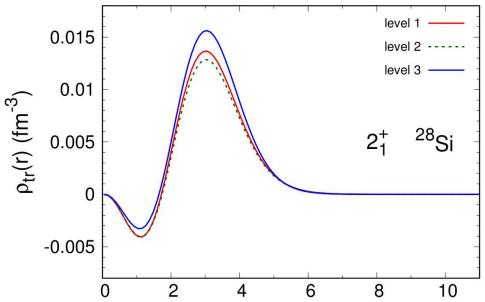

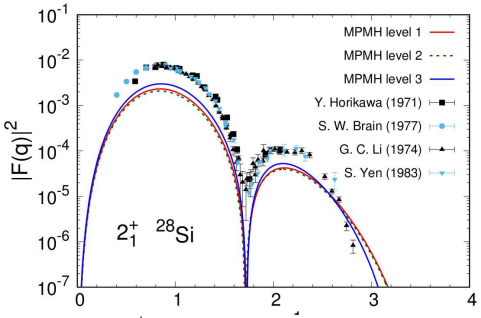

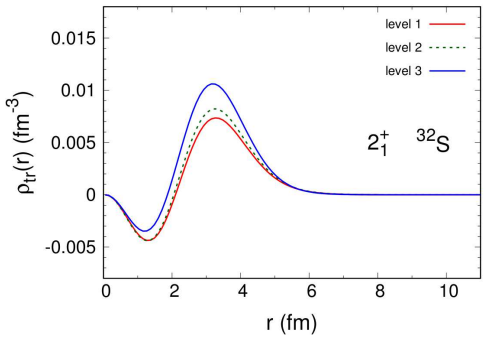

Level 1:
- Factor 4 needed to reach experiment
- Good trend except toward high q

Level 3:
- Factor 2.5 needed to reach experiment
- Improvement of the trend at the tail

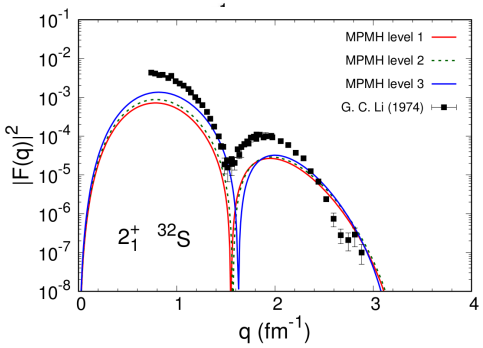

VARIOUS APPLICATIONS WITH THE GOGNY FORCE

Inelastic electron scattering between discrete states: Form factor

Increasing the valence space…

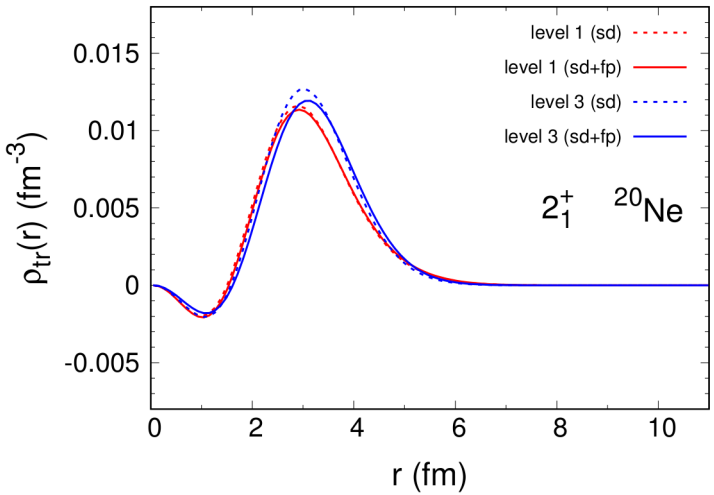

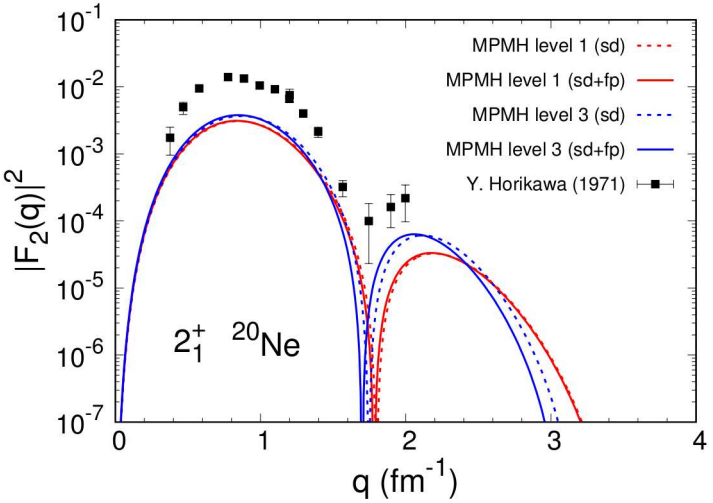

VARIOUS APPLICATIONS WITH THE GOGNY FORCE

Inelastic proton scattering between discrete states

Marc Dupuis
CEA/DAM/DIF

- Transition amplitudes calculated in the DWBA framework

$$T_{fi} \simeq \langle \chi_f^-(\mathbf{k_f}) \Psi_n | \hat{V}_{eff} | \chi_i^+(\mathbf{k_i}) \Psi_0 \rangle$$

- Equations related to the distorted wave $\chi_f^-(\mathbf{k_f})$ and $\chi_i^+(\mathbf{k_i})$

$$\Big(E_i - T_0 + \langle \Psi_0 | \hat{V}_{eff} | \Psi_0 \rangle\Big) \chi_i^+(\mathbf{k_i}) = 0$$

$$\Big(E_f - T_0 + \langle \Psi_0 | \hat{V}_{eff}^\dagger | \Psi_0 \rangle\Big) \chi_f^-(\mathbf{k_f}) = 0$$

- Transition and optical potentials $\hat{U}_{n0} \equiv \langle \Psi_n | \hat{V}_{eff} | \Psi_0 \rangle$ and $\hat{U}_{00} \equiv \langle \Psi_0 | \hat{V}_{eff} | \Psi_0 \rangle$

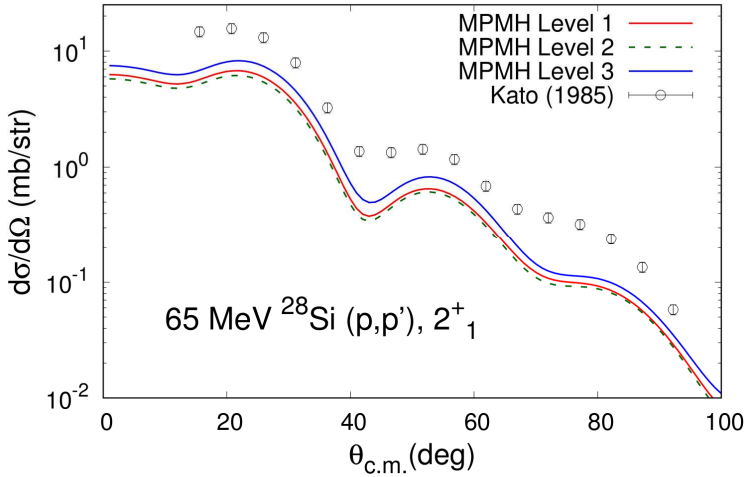

$$\hat{U}_{nm} = \frac{1}{2} \sum_{ij\ kk'} \langle k'j | \hat{V}_{eff} | \widetilde{ki} \rangle \langle \Psi_n | a_j^\dagger a_i | \Psi_m \rangle a_{k'}^\dagger a_k$$

From MPMH:

$$\rho_{\alpha\alpha'}^{nn'} = \langle \psi_{n'} | a_{\alpha'}^\dagger a_\alpha | \psi_n \rangle$$

VARIOUS APPLICATIONS WITH THE GOGNY FORCE

Level 1 description of odd nuclei (also feasable for odd-odd)

- **Spin of ground states**

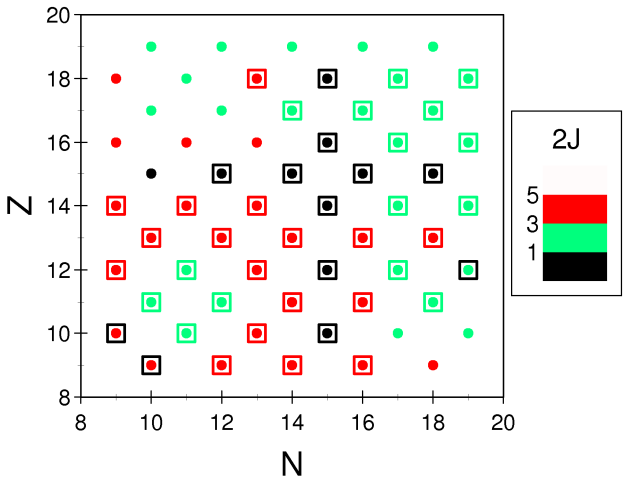

^{19}F - ^{19}N cases:

✓ Inversion between the ground state and the first excited state.

✓ Opening of the core allows to recover the experimental data

⟹ Importance of core polarization

- **First excited states**

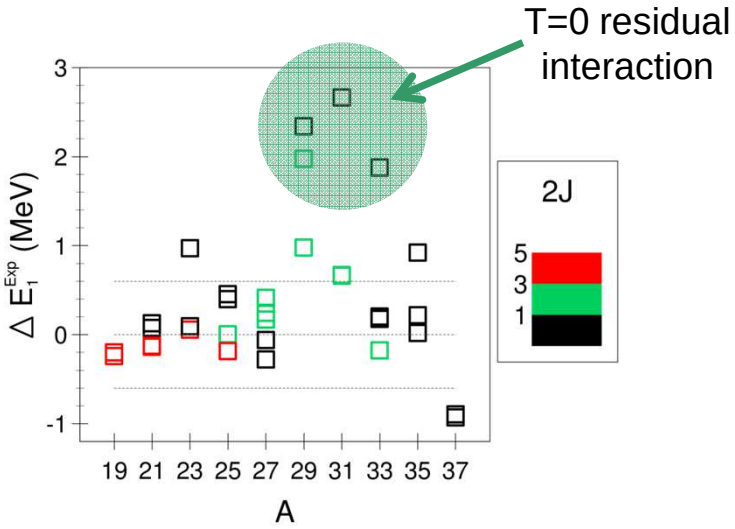

- **Example: Na isotopic chain**

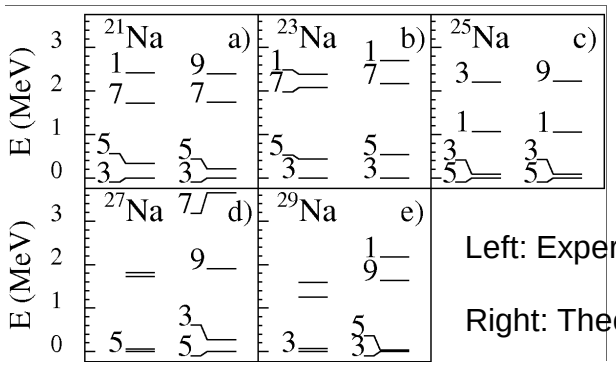

Left: Experiment

Right: Theory

SELF-CONSISTENT MULTIPARTICLE-MULTIHOLE CONFIGURATION MIXING

I. General overview
- ✓ General context
- ✓ Link with Green's functions: Exact solution
- ✓ Optimization of orbitals: Truncated solution

II. Numerical algorithm with orbital optimization
- ✓ ^{12}C test nucleus

III. Various applications with the Gogny force
- ✓ Structure: sd-shell nuclei
- ✓ Reactions: (e,e') and (p,p') inelastic scattering

IV. Conclusion and perspectives
- ✓ Derivation of an effective interaction
- ✓ Complex scaling
- ✓ Fitting of a generalized Gogny interaction
- ✓ Effective operators

CONCLUSION AND PERSPECTIVES – WORK IN PROGRESS

Guillaume Hupin
Postdoc at CEA/DAM/DIF

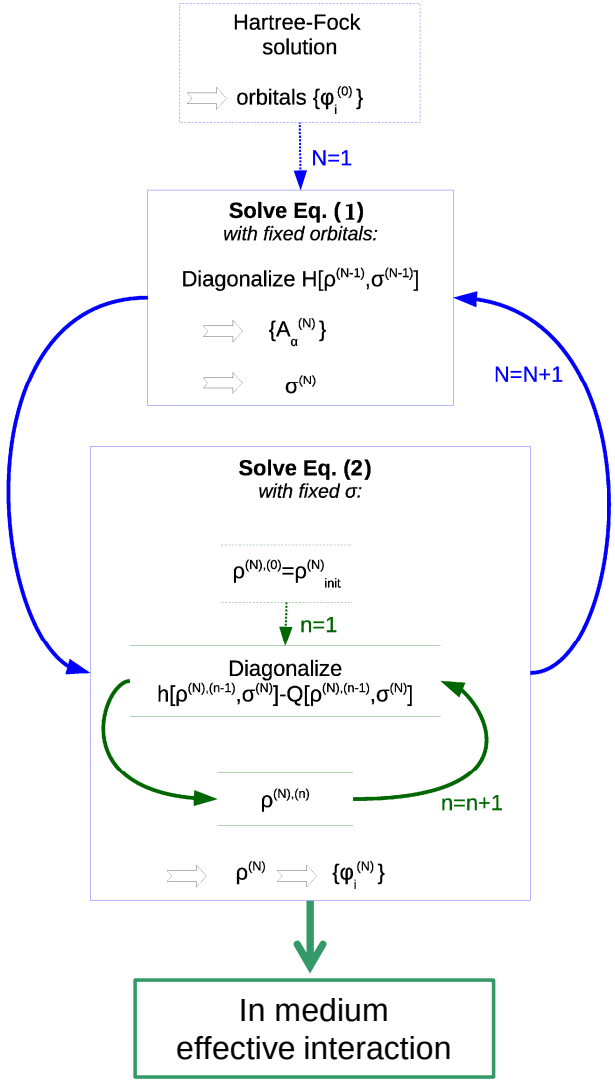

Derivation of an effective interaction

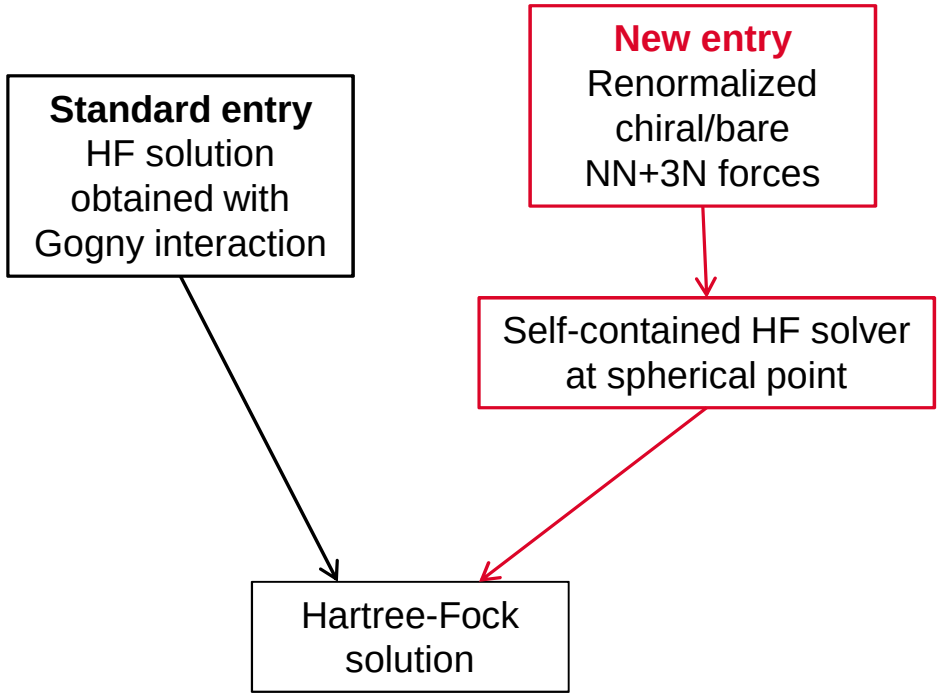

⟹ MPMH configurations introduced at a given order of excitation

CONCLUSION AND PERSPECTIVES– WORK IN PROGRESS

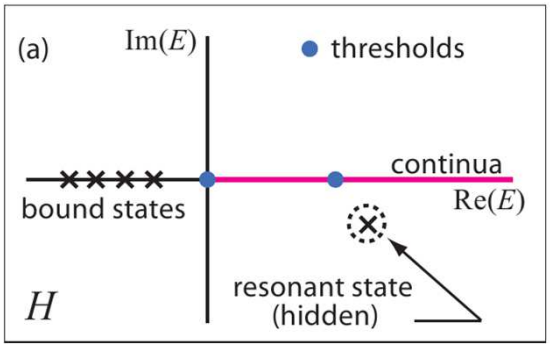

Complex scaling

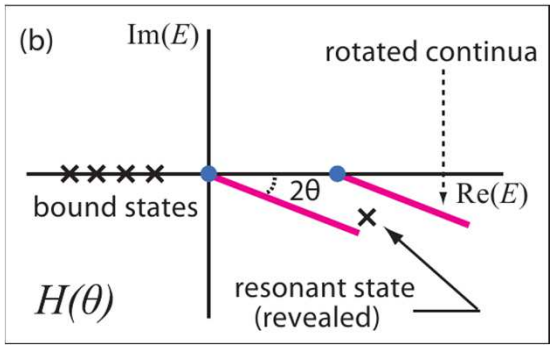

The complex scaling and the resonance states

$$H(r) = T + V(r) \Rightarrow \begin{matrix} H(\theta) = e^{-2i\theta}T + V\left(re^{i\theta}\right) \\ H(r) = U(\theta)H(r)U(\theta)^{-1} \end{matrix}$$

U(θ) is a non-unitary operator of the rotation in the complex plane

Underlying Aguilar-Balslev-Combes theorem: the resonant states of the original Hamiltonian are invariant and the non-resonant scattering states are rotated and distributed on a 2θ ray that cuts the complex energy plane with a corresponding threshold being the rotation point.

Solve the Schrödinger equation in a L^2 basis (i.e. HO, MPMH orbitals…)

$$H(r,\theta)\psi(r,\theta) = (E + i\Gamma)\psi(r,\theta)$$

Energie Demi-vie

En pratique

$$\int \phi_n(r)V\left(re^{i\theta}\right)\phi^{n'}(r)r^2dr = e^{-i3\theta}\int \phi_n\left(re^{i\theta}\right)V(r)\phi^{n'}\left(re^{-i\theta}\right)r^2dr$$

Analytic for Gaussian

CONCLUSION AND PERSPECTIVES– WORK IN PROGRESS

Schematic case: the deuteron

Collaboration with R. Lazauskas and J. Carbonell

- Use of an HO basis in Jacobi coordinates
- Diagonalization in the deuteron channel

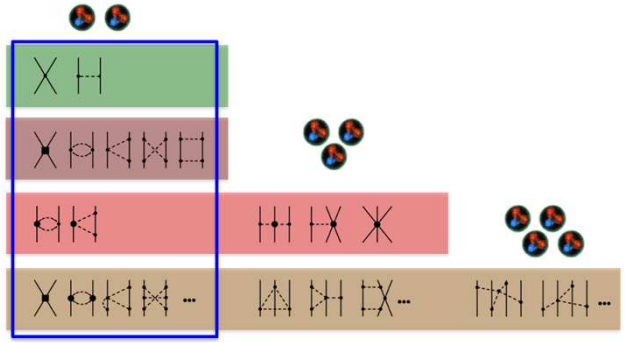

Malfliet-Tjon

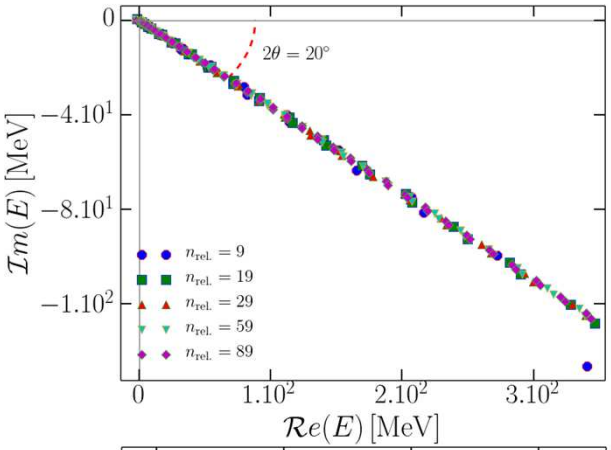

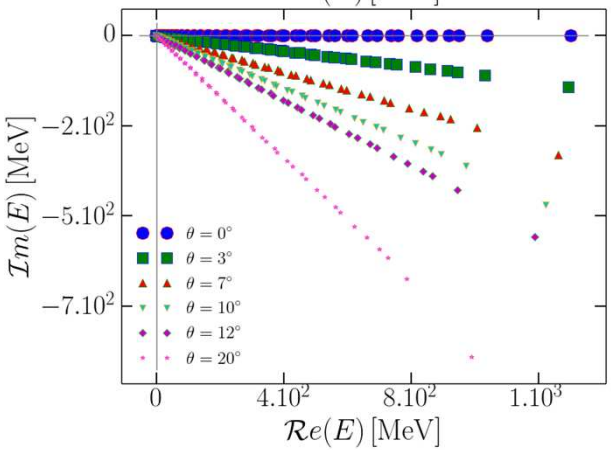

N^{3}LO

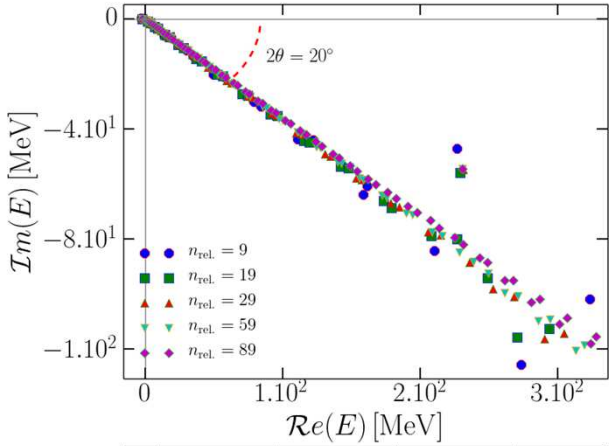

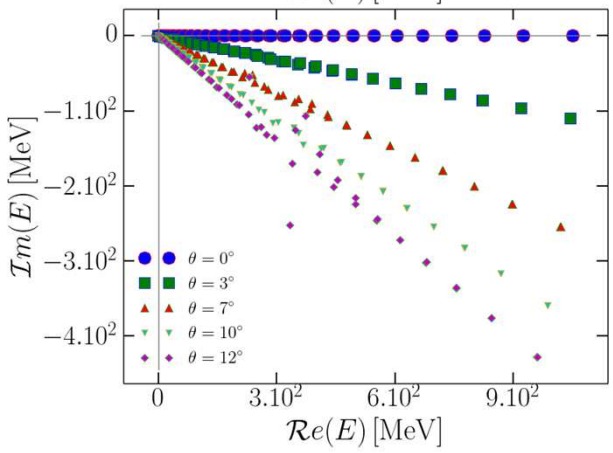

Generalization of the MPMH configuration mixing approach to symmetric non-hermitian complex matrices !

CONCLUSION AND PERSPECTIVES– WORK IN PROGRESS

Rémi Bernard
Postdoc at CEA/DAM/DIF

Toward a generalized Gogny interaction

- **D1 family**

$$V_{12}(\rho) = \sum_{j=1}^{2} \left(W_j + B_j P_\sigma - H_j P_\tau - M_j P_\sigma P_\tau\right) e^{-(\vec{r_1}-\vec{r_2})^2/\mu_j^2}$$
$$+t_3 \left(1 + x_0 P_\sigma\right)\ \delta\left(\vec{r_1} - \vec{r_2}\right)\ \rho^\alpha\left(\tfrac{\vec{r_1}+\vec{r_2}}{2}\right)$$
$$+iW_{LS}\ \overleftarrow{\nabla}_{12}\ \delta\left(\vec{r_1} - \vec{r_2}\right) \wedge \overrightarrow{\nabla}_{12}\left(\vec{\sigma}_1 + \vec{\sigma}_2\right)$$

- **D2 family**

$$V_{\text{dens}}^{D1} = t_0 \left(1 + x_0 P_\sigma\right) \delta\left(\vec{r}_1 - \vec{r}_2\right) \rho^\alpha \left(\frac{\vec{r}_1 + \vec{r}_2}{2}\right)$$

$$V_{\text{dens}}^{D2} = \left(W_3 + B_3 P_\sigma - H_3 P_\tau - M_3 P_\sigma P_\tau\right) \times \frac{e^{-\frac{(\vec{r}_1 - \vec{r}_2)^2}{\mu_3^2}}}{(\mu_3\sqrt{\pi})^3} \frac{\rho^\alpha(\vec{r}_1) + \rho^\alpha(\vec{r}_2)}{2}$$

(F. Chappert et al., PRC91, 034312(2015))

- **DG family**

  - ✓ Collaboration with M. Anguiano, G. Cò and M. Martini
  - ✓ Finite range spin-orbit
  - ✓ Finite range tensor

⟹ **Use of results obtained from the effective interaction derived from bare/chiral interaction + MPMH renormalization**

CONCLUSION AND PERSPECTIVES– WORK IN PROGRESS

Caroline Robin
PhD at CEA/DAM/DIF
Postdoc at WMU

Building of effective operators

- Collaboration with Caroline Robin

- How to take into account the propagation in the Q-subspace within the MPMH configuration mixing?

  $\Longrightarrow$ Interplay between the N-body method and the effective interaction